Geographic divergence and the genomic basis of reproductive diapause in *Drosophila triauraria*

Takako Fujichika[1], Yuki Aoyama[1], Moe Onuma[1], Masafumi Nozawa[1, 2], Aya Takahashi[1, 2]

[1] Department of Biological Sciences, Tokyo Metropolitan University, Japan
[2] Research Center for Genomics and Bioinformatics, Tokyo Metropolitan University, Japan

*Correspondence: ayat@tmu.ac.jp

Abstract

Adjusting reproduction timing to environmental cues is essential for lifetime fitness. In many insects, reproductive diapause shows clinal variation along environmental gradients such as photoperiod and temperature. How such continuous trait variation may be encoded at the molecular level and maintained in the presence of gene flow remains largely elusive. The fruit fly *Drosophila triauraria*, distributed across a wide latitudinal range of the Japanese archipelago. Northern strains exhibit a strong photoperiodic reproductive diapause in females, whereas southern strains fail to arrest ovarian development even under short-day conditions at low temperatures. These distinct phenotypes and the presumable clinal variation in between, provide an ideal opportunity to examine the molecular basis of latitudinal divergence. We first investigated diapause induction in both females and males from previously reported and newly tested strains collected from the regions spanning ~26–43°N. The assessment revealed continuous geographic variation in sensitivity to photoperiod and temperature. We then analyzed the whole-genome sequences of 21 strains, including 14 newly sequenced, to identify genomic regions underlying this divergence. In addition to the conventional F_{ST} analysis, we applied a "monophyletic window" approach suitable for limited sample sizes. The analysis identified a candidate region containing putative E-box and TER-box sequence motifs of the *timeless* (*tim*) gene, which has been previously implicated in diapause regulation in multiple insect species. The quantitative PCR analysis further supported a partial association between the *tim* expression and the incidence of female diapause. These findings reinforce the growing evidence for a role of circadian clock genes in the adaptive regulation of reproductive diapause and demonstrate the utility of tree-based approaches for detecting genomic regions of geographic divergence.

INTRODUCTION

Adjusting internal physiological states to environmental fluctuations is essential for survival and reproductive success. Traits related to the sensitivity to environmental cues or the magnitude of physiological responses often maintain polymorphisms due to fluctuating or unpredictable fitness outcomes (e.g., Johnson et al., 2023). Such traits may also exhibit intraspecific clinal variation when key environmental factors follow a continuous geographical gradient (reviewed in Hut et al., 2013; Mayekar et al., 2022). Sensitivity to photoperiod and temperature cues that induce diapause in insects is a well-documented example (reviewed in Bradshaw & Holzapfel, 2007; Denlinger, 2023). Despite decades of studies using various insect species, the molecular mechanisms that enable continuous variation in diapause induction along clinal environmental gradients, and the processes that maintain such variation in the presence of gene flow, remain elusive.

Many studies have attempted to identify loci involved in the photoperiodic regulation of diapause across clinal populations to tackle this question. In *Drosophila melanogaster*, specific genes with large effects have been identified, such as *ls-tim* in European populations (Tauber et al., 2007) and *couch potato* in North America (Schmitt et al., 2008). However, these associations appear inconsistent across different geographic regions (Lee et al., 2011; Zonato et al., 2016; 2018), suggesting a polygenic nature of the phenotype (Bradshaw et al., 2012; Laruson et al., 2020; Barghi et al., 2020). Recent genomic resequencing studies, comparing population differentiation or conducting large-scale phenotype-genotype association analyses, have identified additional candidate genes in various insects, many of which are related to circadian regulations (Kozak et al., 2019; Pruisscher et al., 2021; Lindestad et al., 2022; Yu et al., 2023; Zheng et al., 2025). Although single genetic variants rarely explain the full extent of phenotypic variation in many cases (e.g., Pruisscher et al., 2018; Lindestad et al., 2024), the association between the circadian clock and photoperiodic regulation is widely recognized. Whether this association represents a consistent pattern across diverse insect species requires further investigation. At the same time, despite advances in genomic technologies, collecting sufficiently large sample sizes across broad geographic ranges, alongside phenotypic assays and genome sequencing, continues to be a significant challenge.

Drosophila species, widely accepted to have originated in tropical regions, have expanded to occupy habitats spanning a wide latitudinal range (Throckmorton, 1975; Lemeunier et al., 1986). Their migratory ability has also facilitated the expansion of habitats within species, providing opportunities to investigate both shared and convergent genetic bases of clinal variation. Because of the direct fitness consequences, clinal variation in reproductive diapause, in which reproduction is arrested under unfavorable environmental conditions, is documented in multiple

Drosophila species inhabiting temperate to subarctic regions. The diapause incidence increases with latitude in many of these species, reflecting local adaptation despite ongoing gene flow. For example, diapause incidence varies with latitude between ~35–70°N in *D. montana* (Tyukmaeva et al., 2020; Lankinen et al., 2023) and *D. littoralis* (Lankinen, 1986), and between ~34–43°N in *D. auraria* (Minami & Kimura, 1980; Kimura, 1984; Pittendrigh & Takamura, 1987) and *D. lacertosa* (Ichijo, 1986). Similarly, clinal variation of diapause incidence has been intensively studied in *D. melanogaster* along the eastern coast of North America (~25–45°N) and Europe (e.g., Schmidt et al., 2007; Tauber et al., 2007).

In this study, we focus on *D. triauraria*, a member of the auraria complex, which inhabits wide latitudinal ranges (~26–43°N) across the Japanese archipelago (Kimura, 1987), comparable to that of *D. melanogaster*. In this species, a strong photoperiodic reproductive diapause has been reported in northern strains, whereas, notably, southern strains fail to arrest ovarian development even under short-day conditions at 15°C (Kimura, 1983; 1988; Yamada & Yamamoto, 2011). These distinct phenotypes, together with the presumable clinal variation in between, provide an ideal opportunity to examine the molecular basis of latitudinal divergence.

Here, we investigate the sensitivity to temperature and photoperiod in reproductive diapause induction in both females and males of *D. triauraria* from mid-latitude regions alongside previously reported and newly tested strains from high- and low-latitude populations. We then examined the degree of divergence from the distribution of a previously described polymorphism in genital morphology (Onuma et al., 2022), and also by a phylogenetic analysis using the whole-genome sequences of the 21 *D. triauraria* strains. Next, to finding signatures of regional divergence, we applied a "monophyletic window" approach, in addition to the conventional F_{ST} analysis. A candidate region contained the *timeless* (*tim*) gene; thus, we conducted quantitative PCR analysis to analyze the association between the *tim* expression and the female reproductive diapause incidence. We discuss the involvement of a circadian clock gene in the adaptive regulation of reproductive diapause in *D. triauraria* and demonstrate the utility of the monophyletic window approach for identifying genomic regions showing geographic divergence.

MATERIALS AND METHODS

Fly strains

The *Drosophila* strains used in this study are described in Table 1. The sampled locations on the map are shown in Figure 1. All strains were maintained at 20ºC under the 15 h light: 9 h dark cycle. All flies were fed with standard corn meal food mixed with yeast, glucose, and agar.

Female diapause assay

Ten virgin females collected within 6 h of eclosion were placed into the food vials and reared under an 8 h light: 16 h dark (8L:16D) or a 16 h light: 8 h dark (16L:8D) cycle, at 12°C, 15°C, and 18°C. Flies were dissected after 21 days at 12°C, 16 days at 15°C, and 14 days at 18°C, according to the timing of sexual maturation inferred from the previous studies (Kimura, 1983; Oguma et al., 1996). The females were dissected in phosphate-buffered saline (PBS), and the ovary images were taken by a CCD camera (DP73, Evident) attached to a microscope (SZX16, Evident). The developmental stages of eggs inside the ovarioles were determined according to King (1970). Diapaused ovaries were defined as those with egg stages 0 to 7 (Figure 2).

Measurements of Accessory gland (AG)

Ten non-mated males collected within 6 h of eclosion were dissected immediately or placed into the food vials and reared under an 8L:16D or 16L:8D light/dark cycle at 12°C for 21 days. The males were dissected in PBS and their accessory glands were fixed in 4% paraformaldehyde (PFA) in PBS for 30 min, followed by three washes in PBST (0.05% Tween 20). The samples were then transferred into PBS. For imaging, 7 µL VectorShield with DAPI (Vector Laboratories) was used for mounting on the slides. Images were taken by a CCD camera (DP73, Evident) attached to an inverted microscope (IX73, Evident). The obtained images were analyzed for area measurement using ImageJ (Schneider et al. 2012).

Male genitalia dissection

Genitalia from 10 males aged 7–10 days were dissected in glycerol after boiling whole bodies in 10% potassium hydroxide at 95°C for more than 10 min. Dissections were performed under a stereomicroscope (SZX7, Evident). Images were acquired using an inverted microscope (IX73, Evident) equipped with a CCD camera (DP73, Evident). Image stacks were processed with CellSens software (Evident) to generate depth-composited TIFF files. Terminology and identification of phallic structures followed Rice et al. (2019) and Onuma et al. (2022) for *D. triauraria*.

Genome sequencing

Genomic DNA was extracted from 40 individuals (20 males and 20 females) per strain for the

146 nine *Drosophila triauraria* strains (SPR23-05, SPR23-09, TM15-38, TM15-57, TM15-67,
147 TM15-92, T544, TTR010, and TMU23-02), along with one *D. biauraria* strain (SPR23-04) and
148 one *D. subauraria* strain (ONM29). DNA extraction was performed using the QIAGEN
149 Genomic-tip 20/G kit (QIAGEN), following the protocol described by Solares et al. (2018).
150 DNA concentrations were quantified using a Qubit dsDNA Quantification Assay Kit
151 (Invitrogen). For each sample, 1 µg of DNA was sent to Filgen, Inc. for library construction and
152 sequencing using a NovaSeq6000 platform with 150 bp paired-end reads.
153 Additionally, genomic DNA was extracted separately from 10 females and 10 males
154 from each of the five *D. triauraria* strains (ONM-15, K445, Jou, Yak2, and Yak3) using the
155 Geno Plus Genomic DNA Extraction Miniprep System (Viogen). DNA samples (50–250 ng per
156 sample) were used for library preparation with the Collibri PCR-free ES DNA Library Prep Kit
157 for Illumina (Invitrogen). Quality assessment of the libraries was performed using an Agilent
158 2100 Bioanalyzer (Agilent Technologies). The libraries were then sent to Macrogen Inc., Korea,
159 for sequencing by using a HiseqX with 150 bp paired-end reads.
160
161 **Quality control and variant calling of the genomic sequence data**
162
163 Quality control of the sequencing reads was performed using FastQC (Andrews, 2010). Adapter
164 trimming and quality filtering (QC > 30) were conducted using Trim Galore! (Krueger, 2021).
165 Reads were then mapped to the *D. triauraria* reference genome (GCA_014170255.2,
166 RU_Dtri_1.1, NCBI) using Bowtie2 (Langmead & Salzberg, 2012). The mapped reads were
167 sorted using SAMtools (Li et al., 2009), and variant calling was performed using BCFtools
168 v1.18 (Danecek et al., 2021). The quality of the variant calling process was assessed using
169 MultiQC (Ewels et al., 2016) based on the BCFtools v1.18 output. Post-calling variant filtration
170 was performed using BCFtools v1.18. Variants with QUAL ≤ 10, DP > 120, or MQBZ < -3
171 were filtered out, and the remaining variants were output in variant call format (VCF).
172
173 **Maximum likelihood tree construction**
174
175 A FASTA file for each strain was constructed by replacing the reference sequence with the
176 single-nucleotide polymorphisms and deletions (replaced by "-") in the variant call format
177 (VCF) file. The FASTA files from all strains were merged (alignment kept from the original VCF
178 file) and converted to PHYLIP format. Maximum likelihood phylogenetic trees were constructed
179 using IQ-TREE (Minh et al., 2013; 2020; Nguyen et al., 2015) with ultrafast bootstrap
180 (UFBoot) analysis (1,000 replicates) and the GTR+G+I substitution model. Gaps were removed
181 prior to running IQ-TREE. To construct trees from specific 5 kb windows, the focal regions

were extracted from the merged FASTA file using SeqKit2 (Shen et al., 2024), in prior to PHYLIP conversion.

Monophyletic window analysis by maximum parsimony tree construction

To conduct a genome-wide sliding window analysis, VCF files from all strains were directly merged (without first constructing FASTA files). The merged VCF file was then divided into 5 kb windows with a 1 kb step size using BCFtools v1.18, and converted to PHYLIP format using vcf2phylip.py (Ortiz, 2019). MPBoot v1.1 (Hoang et al., 2018) was used to generate maximum parsimony phylogenetic trees from each window with 1,000 UFBoot replicates. Monophyly of a particular latitudinal group of strains was analyzed using ape 5.0 (Paradis & Schliep, 2019) and phangorn (Schliep, 2011) packages in R (R core team, 2025). Windows with trees containing monophyletic inner branches with UFBoot values ≥ 90 were considered as candidate genomic regions. The phylogenetic trees were visualized and examined using FigTree v1.4.4 (Rambaut, 2018). Other window sizes (10, 20, and 100 kb) were also analyzed for comparisons. To identify genes within the candidate regions, a local BLASTN search (Altschul et al., 1990) using BLAST v2.15.0 (Camacho et al., 2009) was conducted against the *D. melanogaster* transcripts (GCF_000001215.4_Release_6_plus_ISO1_MT_rna.fna.gz), retrieving the hits with E-values < 0.01.

Population structure and genetic differentiation analysis

Population genetic structure was inferred using the ADMIXTURE software (Alexander et al., 2009). Prior to analysis, genotype data were filtered using PLINK v1.90 (Purcell et al., 2007), removing variants with a missing genotype rate greater than 10% and a minor allele frequency below 5%. Only biallelic SNPs located on major autosomes were retained, and variants on unplaced scaffolds were excluded. To minimize linkage disequilibrium, SNP pruning was conducted using the --indep-pairwise 50 10 0.2 setting. ADMIXTURE analysis was performed with values of K ranging from 1 to 6, and cross-validation error values were used to determine the best-fit number of clusters.

To assess genetic differentiation between groups, Weir and Cockerham's F_{ST} value (Weir and Cockerham, 1984) was calculated using VCFtools (Danecek et al., 2011) for each 5 kb window. The weighted F_{ST} statistic was used to account for varying sample sizes. The results were visualized in R using the ggplot2 package (Wickham, 2016).

Sanger sequencing of the two adjacent monophyletic windows (6 kb) including *tim*

218 Genomic DNA was extracted from a single female using the NucleoSpin DNA Extraction Kit
219 (Macherey-Nagel). PCR amplification of the 6 kb region was performed using KAPA HiFi
220 HotStart Ready Mix (KAPA Biosystems) or Takara Ex Premier DNA Polymerase (Takara Bio).
221 Two sets of primer pairs were used: 1) 5'-CAGTGCTGATAAACCCCCTTACCTA- 3' or 5'-
222 CACTTGGTTATGAAAGCCCTAACCT- 3' and 5'-GCCAGTTGTAGGTACTTCTCCTCCT- 3';
223 2) 5'-AAATACCGGTTATGGACTGGTTACTAGC- 3' and 5'-
224 AAGTCCTCCAAGAGGATGCCATAATAGT- 3'. PCR products were purified using AMPure
225 XP beads (Beckman Coulter) or QIAquick Gel Extraction Kit (QIAGEN). Sanger sequencing
226 was performed using BigDye Terminator v3.1 Cycle Sequencing Kit (Applied Biosystems,
227 Thermo Fisher Scientific) and ABI 3130xl Genetic Analyzer (Applied Biosystems, Thermo
228 Fisher Scientific). Sequence assembly was conducted using BioEdit (Hall, 1999), and the
229 resulting FASTA files were compiled and aligned using MEGA7 (Kumar et al., 2016). The
230 heterozygotes were replaced by the reference sequence manually or using Mitsucal (Suzuki et
231 al., 2018).
232 Transcript models of *tim* were built by aligning a publicly available ovary transcripts
233 (SRR11780982) to the reference genome (GCA_014170255.2, RU_Dtri_1.1, NCBI) using
234 HISAT2 (Kim et al., 2019). Adapter trimming and quality filtering (QC > 30) were conducted
235 using Trim Galore! in prior to alignment. The aligned reads were sorted into BAM files with
236 SAMtools and assembled into transcripts using StringTie (Pertea et al., 2015). Open reading
237 frames (ORFs) were predicted with TransDecoder (Haas et al. 2013) with a minimum length of
238 50 amino acids and subsequently filtered by BLASTP against *D. melanogaster* protein
239 sequences (FlyBase dmel-all-translation-r6.36.fasta). BLASTP hits were used to retain only
240 ORFs with significant matches (E-value < 1e-10).
241
242 **3' Rapid amplification of cDNA ends (3' RACE) of *tim* isoforms**
243
244 One hundred heads from *D. triauraria* females reared at 20°C under a 15L:9D light/dark cycle
245 were flash-frozen in liquid nitrogen at Zeitgeber-time (ZT)4, corresponding to 4 h after lights
246 on. Total RNA was extracted using the PureLink RNA Mini Kit with TRIzol Reagent (Thermo
247 Fisher Scientific). RNA concentration was measured using a NanoDrop 2000 spectrophotometer
248 (Thermo Fisher Scientific). cDNA synthesis was performed using PrimeScript III Reverse
249 Transcriptase (Takara Bio) with 1 μg of total RNA as a template. The oligo (dT) primer was
250 used at a final concentration of 100 pmol/μL. PCR amplification was carried out using DNA Ex
251 Premier Polymerase (Takara Bio) with 5'-
252 GAGCTCAAGCTTAATCTGTTAAAAGAGTTTACAGTGG-3' and 5'-
253 CCAGTGAGCAGAGTGACGAGGACTCGAGCTCAAGCTTTTTTTTTTTTTTTTT-3'. PCR

254 products were analyzed by agarose gel electrophoresis, and target bands (800–1,000 bp and
255 3,000–3500 bp) were excised and purified using NucleoSpin Gel and PCR Clean-up Kit (Takara
256 Bio). The purified DNA fragments were cloned into the pBluescript II SK(+) vector (Agilent
257 Technologies). The vector and PCR products were digested by NotI and treated with shrimp
258 alkaline phosphatase (SAP) for dephosphorylation, followed by ligation using T4 DNA Ligase
259 (Takara Bio). The ligated plasmids were transformed into competent *E. coli* cells. Plasmid DNA
260 was extracted from colonies containing plasmids with a PCR product insertion using Cica
261 Geneus Plasmid Kit (Kanto Chemical). The inserted PCR products were then subjected to
262 Sanger sequencing as described above.
263
264 **Quantification of clock genes or *tim* isoforms transcription level**
265
266 Ten virgin females of ONMA20-3 were collected within 6 h of eclosion and reared in food vials
267 (10 individuals per vial) under an 8L:16D or 16L:8D light/dark cycle at 12°C. After 7 days, the
268 females were immediately frozen in liquid nitrogen every 4 h and stored at -80°C. The same
269 protocol was applied to 15 additional strains, except that the samples were collected at 8 h and
270 16 h after lights on under the respective 8L:16D or 16L:8D light/dark cycle.
271 To extract RNA, 10 frozen heads per sample were detached by vortexing for 5 seconds
272 and placed into 2 mL microtubes containing 400 µL TRIzol Reagent and 1.2 mm (diameter)
273 zirconia-silica beads. Tubes were shaken at 3,200 rpm for 2 min using a Beads Crusher µT-12
274 (Taitec). Chloroform (160 µL) was added, and total RNA was purified using the silica-gel-based
275 method of Boom et al. (1990). First-strand cDNA was synthesized from 70 ng total RNA using
276 the PrimeScript RT Reagent Kit with gDNA Eraser (Takara Bio).
277 Realtime reverse transcription quantitative PCR (RT-qPCR) was conducted using
278 TBGreen Premix Ex Taq II (Tli RNaseH Plus, Takara Bio) in a total reaction volume of 12.5
279 µL. Each reaction contained 6.25 µL of TBGreen Premix, 2 µL of the 3-fold diluted cDNA
280 sample, and 10 pmol each of forward and reverse primers (*tim-L*: 5'-
281 CCCGCATGTATGTAAGCGATG- 3' and 5'-AACTCGGATCTGGGATCTGCT- 3', *tim-sc*: 5'-
282 TGAACACTCCTCCAAAGTCACC- 3' and 5'-GCATCTTAATCCTTACCAAATGG- 3').
283 Reactions were performed using the Dice Real Time System II thermal cycler (Takara Bio). The
284 standard curves generated from 5-fold serial dilutions of an arbitrarily selected sample (the third
285 replicate of the OEB12 samples collected at ZT16 under 16L:8D light/dark cycle) were used.
286 Each sample was analyzed in technical duplicate, with three biological replicates for each
287 condition.
288
289
290 **RESULTS**

Geographic variation in female diapause induction

Previous studies have reported a strong photoperiodic induction of reproductive diapause in females of *D. triauraria* from subarctic regions (42–44°N) and the contrasting non-diapausing phenotype of those from subtropical regions (26–28°N) of the Japanese archipelago (Kimura, 1983; 1988; Kimura & Yoshida, 1995; Yamada & Yamamoto, 2011). Strains from the template regions in between exhibited various levels of photoperiodic induction of reproductive diapause at 15°C (Kimura, 1983; 1988). To investigate the geographic variation in photoperiodic responses across temperatures, we measured the proportion of ovaries in reproductive diapause at 12°C, 15°C, and 18°C under either an 8L:16D or 16L:8D light/dark cycle using 21 strains from high- to low-latitude localities (Table 1, Figure 3).

Consistent with the previous studies, the strains from low-latitude regions showed almost no diapause incidence under any condition, showing continuous ovarian development. In contrast, strains from high-latitude regions induced diapause under short-day conditions in a temperature-dependent manner but went into reproductive mode under the long-day photoperiod regardless of temperature. Reproducing under long-day conditions at low temperature may be an adaptive strategy to cope with short summers in high-latitude localities.

Mid-latitude strains showed photoperiod-dependent diapause induction at 15°C and 18°C, like high-latitude strains. However, at 12°C, approximately half of the females induced reproductive diapause under the long-day condition. These results suggest that although mid-latitude strains respond to photoperiods like high-latitude strains, their photoperiodic response at low temperature is reduced, indicating a higher sensitivity to temperature. Three strains from Yakushima Island, which is known for its unique climate including subtropical in the coastal area to near subarctic in the mountainous ranges > 1,800 m, exhibited variable extent of diapause induction under all temperature conditions.

Diapause induction in males

While reproductive diapause is more pronounced in females compared to males in *Drosophila* species, males also exhibit reduced reproductive activity under unfavorable conditions (Kimura, 1988; Kubrak et al., 2016; Ala-Honkola et al., 2020). The cost of reproduction typically differs between males and females (Bateman, 1948; Trivers, 1972); therefore, they may apply different criteria when allocating energy to reproduction. We investigated this possibility by examining male reproductive status under the 8L:16D or 16L:8D light/dark cycle at 12°C using 12 strains (four each from high-, mid-, and low-latitude populations). Reduction of testis and accessory

gland size at low temperature and short photoperiod has been reported in *D. melanogaster* (Kubrak et al., 2016). However, unlike egg development in ovarioles, which has a checkpoint prior to the initiation of vitellogenesis, when environmental condition is assessed before investigating energy into egg production (Giorgi & Deri, 1976; Drummond-Barbosa & Spradling, 2001), there is no explicit point of arrest in male reproductive organs. Thus, we measured the size of accessory glands, where costly proteins are produced to be injected into the female reproductive tract during copulation.

The accessory gland sizes were measured from the males of all 12 strains kept 21 days after eclosion under the 8L:16D or 16L:8D light/dark cycle at 12°C (Figure 4A). For comparison, those of newly eclosed males within 6 h of eclosion were also measured and the 95% confidence interval (CI) was calculated from the measurement of all strains except T544 (Figure S1). Because the accessory glands of T544 males were significantly larger than those of Jou, OEB12, and OKNG12-6, the 95% CI was calculated separately for this strain. In this study, the males were conservatively classified as reproductively arrested if their accessory gland size was below the upper 95% CI limit of the newly eclosed males. Individuals with accessory gland sizes exceeding this threshold were classified as developing.

The proportion of males under reproductive arrest are shown in Figure 4B. Unlike females, no male in any of the 12 strains met the criteria of reproductive arrest under the 16L:8D light/dark cycle. Their accessory gland sizes not only exceeded the upper 95% CI limit of the newly eclosed males but also showed substantial growth in all strains (Figure 4A and Figure S1). Under the 8L:16D light/dark cycle, some individuals from the high- and mid-latitude strains went into reproductive arrest; however, the proportion did not exceed 60% in any strain, even under the condition where most of females from these regions entered reproductive diapause. These results suggest a weaker suppression of reproduction in males compared to females under unfavorable conditions. Consistent with the reproductive status of the females at 12°C, the males from low-latitude regions did not enter reproductive arrest under either photoperiod.

Intraspecific variation in male genital morphology

To assess the degree of divergence among the latitudinal groups within this species, we examined another polymorphic trait related to reproduction. Unlike the diapause-related traits, genital morphology in general is not influenced by environmental factors and is often used for species identification. Different morphological forms of aedeagus appendages have raised considerable debate over species delimitation of *D. triauraria*. Bock & Wheeler (1972) initially described *D. quadraria* from Taiwan as a distinct species based on differences in male genital

morphology, specifically the presence of smaller appendages (dorsolateral claws) compared to those of *D. triauraria* (type specimen from Tokyo, Japan). However, subsequent fertility assays of hybrids (Kimura, 1987; Kim et al., 1989) and molecular phylogenetic analyses (Miyake & Watada, 2007) led to the reclassification of *D. quadraria* as a junior synonym of *D. triauraria* (Watada et al., 2011). Additionally, individuals with similarly small appendages have been reported from the southern islands of Japan (Onuma et al., 2022), further supporting that the observed variation reflects intraspecific rather than interspecific differences.

The morphological variation in aedeagus appendages was classified into two types, N and S (Figure 5 upper panel). Type N is characterized by larger appendages with a narrower space between them compared to type S. Type N corresponds to the originally described form in *D. triauraria* (Bock & Wheeler, 1972), while type S matches the form from Nansei (Ryukyu) Islands (Onuma et al., 2022), corresponding to the low-latitude region in this study. Genital morphology was examined in 10 males per strain. The strains from southern Japan (low-latitude, Yakushima, and two mid-latitude strains) possessed only type S, whereas most mid- and high-latitude strains included both types (Figure 5 lower panel). Although a weak differentiation between northern and southern populations was apparent, discrepancies between the genital morphology and diapause phenotype suggest that these traits segregate independently, reflecting long-term gene flow across geographic regions.

Genomic phylogeny and geographic differentiation in *D. triauraria*

Whole-genome sequences were analyzed to further investigate the overall genetic differentiation among *D. triauraria* strains and the relationship to three other species from the auraria complex. Short-read sequencing data were generated from 14 *D. triauraria*, one *D. subauraria*, and one *D. biauraria* strains, and additional data for seven *D. triauraria* and four *D. auraria* strains were retrieved from the NCBI Sequence Read Archive (SRA) (Table 1). Phylogenetic analysis using a maximum-likelihood tree based on the whole-genome sequences revealed that strains from *D. triauraria* and *D. auraria* formed separate clades (Figure 6). Within *D. triauraria*, a weak north to south clinal differentiation was observed, with southern population being closer to the other three species of the auraria complex. The low-latitude strains formed a single cluster, whereas strains within each of the high-, mid-latitude, and Yakushima regions did not.

An ADMIXTURE analysis was also conducted to investigate geographic structure among the strains. However, the cross-validation error was consistently lowest at K = 1 across all chromosomes, even when strains from other species were included (Figure S2A). Further analysis at K = 2, which had the second-lowest cross-validation error, did not reveal any clear patterns of regional or species-level clustering (Figure S2B). These results indicate that, despite

the clinal variation in diapause induction thresholds (Figure 3), these *D. triauraria* populations lack strong genomic differentiation by geography, consistent with long-term gene flow across regions.

Identification of genomic regions differentiated among geographic populations

The genital morphology polymorphism and the whole-genome phylogeny suggest that divergence among latitudinal groups at loci regulating reproductive diapause is likely to be maintained despite gene flow. Such loci should therefore exhibit signatures of divergence among latitudinal groups, in contrast to the rest of the genome. To identify these regions, we employed a tree-based method, focusing on strains from extremes of the species distribution (high- and low-latitude groups), where diapause phenotypes differ most strongly. The genome was partitioned into 5 kb windows with a 1 kb step size, and the windows were screened for those in which high- and low-latitude strains formed monophyletic clusters with ≥ 90% bootstrap (UFBoot) support. A window size of 5 kb was chosen after comparison with 10, 20, and 100 kb windows, which produced largely consistent UFBoot profiles (Figure 7 and Figure S3), indicating that the 5 kb window provided finer-scale resolution while retaining sufficient phylogenetic signal.

For the high-latitude group, 55 monophyletic windows were detected on the X chromosome, two windows on 2L, and a single window on 3R (Figure 7A and Table S1). The clustered windows on the X chromosome, stretching discontinuously from 29.437 Mb to 30.287 Mb, included the region homologous to *D. melanogaster* Y chromosome (29.7–34.9 Mb, Chang et al., 2023) and therefore almost no coding genes were found (Table S1). Notably, the two windows on 2L included *timeless* (*tim*), which has been implicated for diapause regulation in many insect species (Mathias et al., 2005; Tauber et al., 2007; Sandrelli et al., 2007; Pruisscher et al., 2018; Lindestad et al., 2022; Vaze et al., 2024) and also suggested to be associated with diapause induction in *D. triauraria* (Yamada & Yamamoto, 2011). Sanger resequencing of the two consecutive windows spanning a 6 kb region confirmed the presence of two putative E-box motifs and one TER-box motif (Figure 8), which are critical for the circadian gene regulation (McDonald et al., 2001). The 11 polymorphic sites fixed in the high-latitude group were located in intronic regions outside these motifs.

In the low-latitude group, which does not respond to either photoperiod or temperature, a total of 188 monophyletic windows were located on chromosomes X, 2L, 2R, and 3R (Figure 7B, Table S2). These regions included *eyes shut* (*eys*), known to be involved in temperature entrainment of circadian activity (Sehadova et al., 2009); *nahoda*, which is expressed in egg chambers (Manning et al., 2017); and *Sox100B*; which plays a role in male-

435 specific gonad development (Nanda et al., 2009). The involvement of these genes in the
436 regulation of reproductive diapause has not been implicated.
437 The genome-wide F_{ST} window comparisons are more commonly applied to detect
438 divergent genomic regions between populations. However, F_{ST} estimates can be biased when the
439 sample sizes are small or uneven among regional populations (Whitlock and McCauley, 1999;
440 Willing et al., 2012). To address this, we compared the windows with the highest F_{ST} values to
441 those identified using the tree-based approach (Figure S4 and Figure S5). These comparisons
442 revealed that 93.1% (54 out of 58) of the monophyletic windows in high-latitude strains
443 (including those with the *tim* locus) and 92.0% (173 out of 188) in low-latitude strains
444 overlapped with the top 5% F_{ST} windows. Therefore, the monophyletic windows largely
445 represent a selected subset of the highest F_{ST} windows by an additional criterion of strong
446 bootstrap support for monophyly.
447
448 **Association between the expression of *tim* isoform groups and diapause incidence**
449
450 Multiple *tim* isoforms are expressed in *D. melanogaster* and other species of the *melanogaster*
451 subgroup (Low et al., 2008; Anduaga et al., 2019). These isoforms can be categorized by size:
452 long isoforms (*tim-L*, *tim-cold*), and a short isoform (*tim-sc*). *tim-L* is the canonical isoform,
453 while *tim-cold* and *tim-sc* are more abundant at low temperatures. The roles of these isoforms
454 have been investigated in *D. melanogaster*, variants of the *tim-L* isoform (*ls-tim-* and *s-tim*) are
455 known to regulate diapause induction (Tauber et al., 2007; Sandrelli et al., 2007), and
456 accumulation of TIM-SC under low temperature, short-day condition is implicated in diapause
457 regulation by stabilizing Eyes absent (EYA) (Abrieux et al., 2020).
458 The isoform differences are mostly attributed to alternative splicing downstream of
459 exon 9. Thus, to investigate the presence of these isoforms in *D. triauraria*, we performed 3′
460 RACE using RNA extracted from the heads of females from two strains, ONMA20-3 (high-
461 latitude) and OEB12 (low-latitude). We were able to identify sequences corresponding to the
462 two common isoforms, *tim-L* and *tim-sc*, and designed primers within the terminal exons to
463 quantify the abundance of the long and short isoforms (hereafter referred to as *tim-L* and *tim-sc*
464 isoform groups, respectively) by a realtime RT-qPCR (Figure S6). Although *tim-cold* and *tim-M*
465 were not detected in our 3' RACE analysis, they may still be amplified by the primers targeting
466 the *tim-L* isoform group. It should be noted that other undetected isoforms may also be
467 amplified by the designed primer pairs.
468 The oscillation patterns of *tim-L* and *tim-sc* isoform groups in the heads of females
469 from the ONMA20-3 strain were analyzed under an 8L:16D or 16L:8D light/dark cycle at 12°C
470 (Figure S7). The temporal patterns of *tim-L* expression under both photoperiods largely

coincided with the nuclear accumulation of TIM in the lateral ventral neurons (LN_v) of *D. melanogaster* brain (Shafer et al., 2004), including a possible phase advance at low temperature (Majercak et al., 1999; Anduaga et al., 2019). The overall expression level of *tim-L* isoform group (averaged across six timepoints) was significantly higher under the 16L:8D light/dark cycle than under 8L:16D (*t*-test after hyperbolic arcsine transformation: $t = 14.94$, df = 2, $P < 0.01$), whereas no significant difference was observed between the two cycles in the *tim-sc* isoform group ($t = 3.54$, df = 2, $P = 0.07$).

To investigate whether the differences between the two light conditions in expression of the two isoform groups (particularly *tim-L*, which showed a significant light-dependent difference in ONMA20-3) are associated with diapause incidence at 12°C, the *tim* mRNA abundance was quantified at ZT8 and ZT20 under 8L:16D and 16L:8D in female heads from the high-, mid-, and low-latitude strains (Figure S8A). Two-way ANOVA showed that the *tim-L* expression in the low-latitude strains was significantly lower than in the high-latitude strains under both light conditions and also significantly lower than in the mid-latitude strains under 8L:16D (Figure S8C), suggesting a distinct regulatory mechanism of this isoform group in the low-latitude strains. For the *tim-sc* isoform group, no significant effects were observed except for a difference between the high- and mid-latitude groups under the 8L:16D light/dark cycle (Figure S8B and Figure S8C).

Because the low-latitude strains exhibited no reproductive diapause even under the 8L:16D short-day condition at 12°C and displayed distinct *tim-L* expression profiles, the following association analysis was conducted using only the high- and mid-latitude strains, which showed variable diapause incidence under the 16L:8D long-day condition at 12°C. To explain variation in diapause incidence under 16L:8D, we considered the following model:

$$\Delta_{8L16D\text{-}16L8D} P_{diap} = \beta_0 + \beta_1 \cdot tim\text{-}L_{16L8D} + \beta_2 \cdot tim\text{-}sc_{16L8D} + \beta_3 \cdot \Delta_{16L8D\text{-}8L16D}\, tim\text{-}L + \beta_4 \cdot \Delta_{16L8D\text{-}8L16D}\, tim\text{-}sc + \varepsilon,$$

where $\Delta_{8L16D\text{-}16L8D} P_{diap}$ is the difference in the arcsine-transformed diapause proportions between the 8L:16D and 16L:8D cycles. $tim\text{-}L_{16L8D}$ and $tim\text{-}sc_{16L8D}$ denote the hyperbolic arcsine-transformed relative expression levels under 16L:8D, and $\Delta_{16L8D\text{-}8L16D}\, tim\text{-}L$ and $\Delta_{16L8D\text{-}8L16D}\, tim\text{-}sc$ represent the differences in expression between the two light conditions. Both arcsine and hyperbolic arcsine transformations were applied to normalize values for linear modeling.

We then analyzed the model by the stepwise selection using BIC, which identified the following model as the best-fit model:

$$\Delta_{8L16D\text{-}16L8D} P_{diap} = \beta_0 + \beta_3 \cdot \Delta_{16L8D\text{-}8L16D}\, tim\text{-}L + \varepsilon,$$

with the coefficient estimates shown in Table 2. The result indicates that the differences in *tim-L* expression between the two light conditions are significantly associated with the differences in

diapause incidence at 12°C. The positive regression coefficient indicates that strains with relatively higher *tim-L* expression under the long-day condition (16L:8D) show reduced diapause incidence, suggesting an enhanced reproductive activity at low temperature.

DISCUSSION

Initiating or arresting reproduction is a critical life-history choice with major consequences for lifetime fitness. Like many other insects, *D. triauraria* respond to environmental cues such as temperature and photoperiod to make the choice. We conducted a comprehensive analysis of the female reproductive diapause induction in 21 strains of this species, including both newly tested and previously reported strains collected from across the Japanese archipelago (26.2–43.1°N). Our results revealed that a key difference between the high- and mid-latitude strains lies in their temperature sensitivity under the long-day condition (16L:8D). At 12°C, females from the mid-latitude strains exhibited a higher incidence of reproductive diapause compared to those from the high-latitude strains (Figure 3). This reduced sensitivity to low temperature (i.e., stronger photoperiodic induction of diapause) in the high-latitude strains likely reflects adaptation to northern environments, where reproducing under cooler and shorter summer seasons is essential.

Although direct comparisons between sexes are challenging, our results suggest that females and males from the high- and mid-latitude regions differ in how reproduction activity is modulated by photoperiod and temperature (Figure 3 and Figure 4). This implies that the thresholds for reproductive suppression vary between sexes, potentially reflecting sex-specific life history strategies. In particular, males may maintain investment in reproduction under suboptimal conditions, consistent with the relatively lower energetic cost of reproduction compared to females (Bateman, 1948; Trivers, 1972). Future work should examine the extent to which shared versus sex-specific neuroendocrine pathways and sensory circuits contribute to these differences. Moreover, assessing traits beyond accessory gland development, such as spermatogenesis status and courtship behavior, will be essential for a comprehensive understanding of intersexual variation in reproductive status under unfavorable environmental conditions.

Our whole-genome phylogeny revealed only weak geographic divergence (Figure 6), and the observed discrepancies between genital morphology and diapause phenotype (Figure 5) further suggest that long-term gene flow across geographic regions has generated sufficient recombination to decouple genomic regions associated with different traits. Such genomic decoupling provides an opportunity to identify geographically divergent regions associated with

543 specific phenotypes. To investigate the genetic basis underlying the observed differences in
544 female diapause response, we applied a monophyletic window approach, which imposes a
545 stricter criterion for identifying genomic regions than the standard F_{ST} scans. Although Weir and
546 Cockerham's weighted F_{ST} estimation corrects for sample sizes of the populations (Weir and
547 Cockerham 1984), small and unbalanced samples, as in this study, can introduce false signals of
548 differentiation (Whitlock and McCauley, 1999; Willing et al., 2012). By focusing on genomic
549 windows where the focal group forms a well-supported monophyletic cluster, this approach
550 helps mitigate such biases.

551 For the high-latitude strain group (against all other groups), there were 54 windows of
552 5 kb in size that showed both ≥ 90% bootstrap support for monophyly and F_{ST} values within the
553 top 5% (Figure S5A), located in two separate genomic regions (one additional window on 3R
554 met the monophyly criterion but fell outside the top 5% F_{ST} threshold) (Figure 7A). The two
555 windows on 2L contained *tim*, and a cluster of windows on the X chromosome included few
556 genes (Table S1). For the low-latitude strain group, 173 windows met both the ≥ 90% bootstrap
557 support and top 5% F_{ST} criteria (Figure S5B). These were distributed across more than 20
558 separate genomic regions (Figure 7B). The smaller number of candidate windows in the low-
559 latitude groups could be due to multiple factors: a smaller number of strains, a higher number of
560 regions under selection, inflated F_{ST} threshold in the high-latitude strains due to a dense cluster
561 of high-F_{ST} windows on the X chromosome, or a combination of these factors. We were unable
562 to examine specific candidate regions within the low-latitude group due to these complexities.

563 Our monophyletic window approach does not directly target diapause-associated loci
564 and may capture divergent regions associated with other locally adapted traits. However, among
565 the windows showing strong signals of high-latitude group monophyly, we found a candidate
566 region encompassing the E-box and T-box regulatory motifs of *tim*. Given the implicated role of
567 *tim* in regulating diapause across multiple insect species, including *D. triauraria*, we further
568 investigated the association between *tim* expression levels and reproductive diapause incidence.
569 Using RT-qPCR, the mRNA levels of the long and short isoform groups were quantified. We
570 detected a significant association across strains between the differences in diapause incidence
571 under the long- and short-day photoperiods and the differences of *tim-L* isoform group
572 expression between those light conditions at 12°C. The analysis focused on the high- and mid-
573 latitude strains, as the low-latitude strain exhibited distinct diapause regulation patterns.

574 As in many organisms, circadian rhythms in *Drosophila* are influenced by light,
575 implicating a link between clock genes and photoperiodic regulation (e.g., Denlinger, 2022). *tim*
576 is a core circadian gene whose product, TIM, is bound by the photoreceptor CRYPTOCHROME
577 (CRY) upon light exposure and subsequently degraded by ubiquitination, resulting in light-
578 induced resetting of the circadian clock (Hunter-Ensor et al., 1996; Ceriani et al., 1999; Busza et

579 al., 2004). The primary light-sensitive isoform, *tim-L*, is included in the isoform group for which
580 we observed an association with diapause incidence. The light-insensitive isoforms, *tim-cold*
581 and *tim-sc*, are induced by low temperature (Montelli et al., 2015; Shakhmantsir et al., 2018;
582 Anduaga et al., 2019; Abrieux et al., 2020). Among these isoforms, TIM-SC contributes to the
583 stabilization of EYA, a key seasonal sensor, suggesting that the relative abundances of *tim-L* and
584 *tim-sc* may play a role in diapause induction in females of *D. melanogaster* (Abrieux et al.,
585 2020). There is no evidence from these *D. melanogaster* studies, however, demonstrating a
586 direct effect of *tim-L* on reproductive diapause. Thus, the mechanisms underlying the observed
587 association in our study, where higher *tim-L* expression associates with lower diapause
588 incidence at low temperature, remains unclear at this point. It is also important to note that the
589 TIM protein abundance was not quantified in our study, and the increased mRNA expression
590 observed under the long-day condition could reflect either an enhanced transcription or
591 compensatory response to light-driven protein degradation. Interestingly, unlike *D.*
592 *melanogaster* and related species such as *D. simulans, D. yakuba,* and *D. virilis*, whose *tim*
593 splicing is temperature-sensitive (Anduaga et al., 2019), the cold-tolerant northern species, *D.*
594 *montana*, exhibits photoperiod-sensitive *tim* splicing (Tapanainen et al., 2018). This suggests
595 that the splicing regulation of *tim* isoforms and their functional roles in circadian and diapause
596 pathways may vary considerably across species.
597 In *D. triauraria*, Kimura and Yoshida (1995) analyzed recombinant inbred lines derived
598 from hybrids between a diapausing strain (ONMA20-3) and a non-diapausing strain from
599 Kametoku (28°N), and estimated that three or four loci underly the difference in the photoperiodic
600 response, with at least one located on the X chromosome. More recently, Yamada and Yamamoto
601 (2011) conducted a genetic analysis and reported an association between reproductive diapause
602 incidence and the genetic marker variants at *tim* and *cry*. This analysis was based on genotyping
603 five clock genes (*per*, *tim*, *clk*, *cyc*, and *cry*) in 329 backcrossed individuals derived from a cross
604 between a diapausing strain (ONMA20-3) and a non-diapausing strain (OEB12). The association
605 with *tim* is consistent with our results, further supporting a potential role for this gene in diapause
606 regulation of *D. triauraria*. However, the low marker density (only five loci across the entire
607 genome) limits their mapping resolution. As they also noted, the observed associations could be
608 due to linkage with nearby genes rather than direct effects of *tim* or *cry*. Our higher-resolution
609 approach allows a more targeted investigation of this region and together with the expression
610 analysis, strengthens the case for *tim* as a candidate gene involved in photoperiodic diapause
611 regulation.
612 Consistent with the previous report (Yamada & Yamamoto, 2011), females of low-
613 latitude strains did not exhibit reproductive diapause under any of the tested conditions (Figure
614 3). We further showed that males of these strains also failed to arrest reproduction (Figure 4)

615 and displayed reduced expression of *tim-L* isoform group (Figure S8A). Taken together with the
616 earlier finding that the diapausing phenotype is completely dominant over the non-diapausing
617 type (Yamada & Yamamoto, 2011), these results suggest that the low-latitude strains may carry
618 impaired signaling pathways required for diapause induction. An intriguing evolutionary
619 question that remains unresolved is the ancestry of the phenotype; whether the absence of
620 diapause in the low-latitude strains represents a derived loss of the trait, or alternatively, whether
621 the ability to enter reproductive diapause was an adaptation acquired in the high-latitude
622 populations.
623 It is widely accepted that *Drosophila* species originated in tropical region and later
624 expanded into temperate and subarctic regions (Throckmorton, 1975; Lemeunier et al., 1986). In
625 our whole-genome maximum likelihood tree, the low-latitude and Yakushima strains of *D.*
626 *triauraria* form the basal lineages (Figure 6), consistent with a tropical origin. However, Kimura
627 (1988) argued that adaptation to cool-temperate climates likely preceded speciation within the
628 *auraria* complex. This view was based on the observation that species within the complex do
629 not differ markedly in cold-hardiness. Supporting this hypothesis, three other species in the
630 complex exhibit reproductive diapause phenotypes similar to that of the northern strains of *D.*
631 *triauraria* (Kimura, 1984; Kimura, 1990). Kimura (1988) further proposed that the current
632 subtropical populations of *D. triauraria* may have established through reinvasion from northern,
633 cool-temperate populations, as these subtropical flies are significantly more cold-hardy than
634 sympatric populations of the subtropical or warm-temperate species like *D. rufa* and *D.*
635 *lutescens*. These competing hypotheses, tropical origin with independent acquisition of diapause
636 in the north versus ancestral diapause with secondary loss in the south, remain difficult to
637 reconcile.
638 However, the phylogenetic analysis of the *tim* genomic region, including other species
639 of the auraria complex (Figure S9), does not support a scenario in which the low- and mid-
640 latitude alleles are derived from the high-latitude allele, nor the reverse. Instead, the tree
641 suggests that these alleles have diverged independently from a basal state. Given the likelihood
642 of frequent introgression and incomplete lineage sorting within the *auraria* complex (Miyake &
643 Watada, 2007; Conner et al., 2021), it is plausible that two alleles of early origin associated with
644 diapause regulation have persisted in different geographic regions within *D. triauraria*.
645 Although our analysis is currently confined to a single locus, the results raise the possibility that
646 key diapause-related alleles originated and diverged close to the time of speciation and
647 subsequently underwent differentiation along latitudinal gradients. In light of the polygenic
648 basis of diapause regulation, information from additional loci will be essential to further test and
649 refine this scenario, thereby providing deeper insights into the evolutionary dynamics of
650 adaptive traits evolving across heterogeneous environments.

ACKNOWLEDGEMENTS

We thank KYORIN-Fly stock center for *D. triauraria* stocks and Masahito T. Kimura for *D. triauraria* and *D. biauraria* flies. We are grateful to Koichiro Tamura for fruitful discussions and support. This work was supported by KAKENHI 23K27221 to AT, 24KJ0181 to MO, 22H05073 to MN, and 22KJ2552 to TF. We used ChatGPT-4.0 to assist in correcting errors in script writing.

AUTHOR CONTRIBUTIONS

TF and AT conceived this work. YA and TF analyzed accessory gland. MO and TF analyzed genital morphology. MN obtained genome sequences of five *D. triauraria* strains. TF and AT analyzed data and wrote the manuscript.

DATA AVAILABILITY STATEMENT

Raw sequence reads have been deposited in the SRA under BioProject PRJDB20728, with individual run accession numbers provided in Table 1. Sequences of *tim* isoform groups are available in DDBJ (accession numbers LC882409–LC882412). Sequencing data for the 6 kb *tim* region are deposited in DDBJ (accession numbers LC884490–LC884507)

ORCID

Takako Fujichika https://orcid.org/0009-0000-6330-8668

Moe Onuma https://orcid.org/0000-0002-2971-7289

Masafumi Nozawa https://orcid.org/0000-0003-1580-8312

Aya Takahashi https://orcid.org/0000-0002-8391-7417

REFERENCES

Abrieux, A., Xue, Y., Cai, Y., Lewald, K. M., Nhu Nguyen, H., Zhang, Y., Chiu, J. C. (2020). EYES ABSENT and TIMELESS integrate photoperiodic and temperature cues to regulate seasonal physiology in *Drosophila*. *Proceedings of the National Academy of Sciences of the United States of America*, *117*(26), 15293–15304. https://doi.org/10.1073/pnas.2004262117

Ala-Honkola, O., Kauranen, H., Tyukmaeva, V., Boetzl, F. A., Hoikkala, A., & Schmitt, T. (2020). Diapause affects cuticular hydrocarbon composition and mating behavior of

both sexes in *Drosophila montana*. *Insect Science*, *27*(2), 304–316. https://doi.org/10.1111/1744-7917.12639

Alexander, D. H., Novembre, J., & Lange, K. (2009). Fast model-based estimation of ancestry in unrelated individuals. *Genome Research*, *19*(9), 1655–1664. https://doi.org/10.1101/gr.094052.109

Altschul, S. F., Gish, W., Miller, W., Myers, E. W., & Lipman, D. J. (1990). Basic local alignment search tool. *Journal of Molecular Biology*, *215*(3), 403–410. https://doi.org/10.1016/S0022-2836(05)80360-2

Andrews, S. (2010). FastQC: A Quality Control Tool for High Throughput Sequence Data [Online]. Available at: http://www.bioinformatics.babraham.ac.uk/projects/fastqc/

Anduaga, A. M., Evanta, N., Patop, I. L., Bartok, O., Weiss, R., & Kadener, S. (2019). Thermosensitive alternative splicing senses and mediates temperature adaptation in *Drosophila*. *eLife*, *8*, e44642. https://doi.org/10.7554/eLife.44642

Barghi, N., Hermisson, J., & Schlötterer, C. (2020). Polygenic adaptation: a unifying framework to understand positive selection. *Nature Reviews Genetics*, *21*(12), 769–781. https://doi.org/10.1038/s41576-020-0250-z

Bateman, A. (1948). Intra-sexual selection in *Drosophila*. *Heredity*, *2*, 349–368 https://doi.org/10.1038/hdy.1948.21

Bock, I. R., & Wheeler, M. R. (1972). The *Drosophila melanogaster* species group. *University of Texas Publications*.

Boom, R., Sol, C. J. A., Salimans, M. M., Jansen, C. L., Wertheim-van Dillen P. M. E., & van der Noordaa J. (1990). Rapid and simple method for purification of nucleic acids. *Journal of Clinical Microbiology*, *28*(3) 495–503. https://doi.org/10.1128/jcm.28.3.495-503.1990

Bradshaw, W. E., Emerson, K. J., Catchen, J. M., Cresko, W. A., & Holzapfel, C. M. (2012). Footprints in time: comparative quantitative trait loci mapping of the pitcher-plant mosquito, *Wyeomyia smithii*. *Proceedings of the Royal Society B: Biological Sciences*, *279*(1747), 4551–4558. https://doi.org/10.1098/rspb.2012.1917

Bradshaw, W. E., & Holzapfel, C. M. (2007). Evolution of animal photoperiodism. *Annual Review of Ecology, Evolution, and Systematics, 38*, 1–25. https://doi.org/10.1146/annurev.ecolsys.37.091305.110115

Busza, A., Emery-Le, M., Rosbash, M., & Emery, P. (2004). Roles of the two *Drosophila* CRYPTOCHROME structural domains in circadian photoreception. *Science*, *304*(5676), 1503–1506. https://doi.org/10.1126/science.1096973

Camacho, C., Coulouris, G., Avagyan, V., Ma, N., Papadopoulos, J., Bealer, K., & Madden, T. L. (2009). BLAST+: architecture and applications. *BMC Bioinformatics*, *10*, 421. https://doi.org/10.1186/1471-2105-10-421

Ceriani, M. F., Darlington, T. K., Staknis, D., Más, P., Petti, A. A., Weitz, C. J., & Kay, S. A. (1999). Light-dependent sequestration of TIMELESS by CRYPTOCHROME. *Science, 285*(5427), 553–556. https://doi.org/10.1126/science.285.5427.553

Chang, C. H., Natividad, I. M., & Malik, H. S. (2023). Expansion and loss of sperm nuclear basic protein genes in *Drosophila* correspond with genetic conflicts between sex chromosomes. *eLife*, *12*:e85249. https://doi.org/10.7554/eLife.85249

Conner, W. R., Delaney, E. K., Bronski, M. J., Ginsberg, P. S., Wheeler, T. B., Richardson, K. M., Peckenpaugh, B., Kim, K. J., Watada, M., Hoffmann, A. A., Eisen, M. B., Kopp, A., Cooper, B. S. & Turelli, M. (2021). A phylogeny for the *Drosophila montium* species group: A model clade for comparative analyses. *Molecular Phylogenetics and Evolution*, 158, 107061. https://doi.org/10.1016/j.ympev.2020.107061

Danecek, P., Auton, A., Abecasis, G., Albers, C. A., Banks, E., DePristo, M. A., Handsaker, R. E., Lunter, G., Marth, G. T., Sherry, S. T., McVean, G., Durbin, R., & 1000 Genomes Project Analysis Group. (2011). The variant call format and VCFtools. *Bioinformatics, 27*(15), 2156–2158. https://doi.org/10.1093/bioinformatics/btr330

Danecek P., Bonfield J. K., Liddle J., Marshall J., Ohan V., Pollard M. O., Whitwham A., Keane T., McCarthy S. A., Davies R. M., & Li H. (2021). Twelve years of SAMtools and BCFtools. *GigaScience*, *10*(2), giab008. https://doi.org/10.1093/gigascience/giab008

Denlinger, D. L. (2022). Insect diapause*. Cambridge University Press*.

Denlinger, D. L. (2023). Insect diapause: from a rich history to an exciting future. *Journal of Experimental Biology*, *226*(4): jeb245329. https://doi.org/10.1242/jeb.245329

Drummond-Barbosa, D., & Spradling, A. C. (2001). Stem cells and their progeny respond to nutritional changes during *Drosophila* oogenesis. *Developmental Biology*, *231*(1), 265–278. https://doi.org/10.1006/dbio.2000.0135

Ewels, P., Magnusson, M., Lundin, S., & Käller, M. (2016). MultiQC: summarize analysis results for multiple tools and samples in a single report. *Bioinformatics*, *32*(19), 3047–3048. https://doi.org/10.1093/bioinformatics/btw354

Giorgi, F., & Deri, P. (1976). Cell death in ovarian chambers of *Drosophila melanogaster*. *Journal of Embryology and Experimental Morphology*, *35*(3), 521–533. https://doi.org/10.1242/dev.35.3.521

Haas, B. J., Papanicolaou, A., Yassour, M., Grabherr, M., Blood, P. D., Bowden, J., Couger, M. B., Eccles, D., Li, B., Lieber, M., Macmanes, M. D., Ott, M., Orvis, J., Pochet, N., Strozzi, F., Weeks, N., Westerman, R., William, T., Dewey, C. N., Henschel, R., LeDuc,

R. D., Friedman, N., & Regev, A. (2013). De novo transcript sequence reconstruction from RNA-seq using the Trinity platform for reference generation and analysis. *Nature Protocols*, *8*(8), 1494–1512. https://doi.org/10.1038/nprot.2013.084

Hall, T. A. (1999). BioEdit: a user-friendly biological sequence alignment editor and analysis program for Windows 95/98/NT. *Nucleic Acids Symposium Series*, *41*, 95–98.

Hoang, D. T., Vinh, L. S., Flouri, T., Stamatakis, A., von Haeseler, A., & Minh, B. Q. (2018). MPBoot: Fast phylogenetic maximum parsimony tree inference and bootstrap approximation. *BMC Evolutionary Biology*, *18*(1), 11. https://doi.org/10.1186/s12862-018-1131-3

Hunter-Ensor, M., Ousley, A., & Sehgal, A. (1996). Regulation of the *Drosophila* protein timeless suggests a mechanism for resetting the circadian clock by light. *Cell, 84*(5), 677–685. https://doi.org/10.1016/S0092-8674(00)81046-6

Hut, R. A., Paolucci, S., Dor, R., Kyriacou, C. P., & Daan, S. (2013). Latitudinal clines: an evolutionary view on biological rhythms. *Proceedings of the Royal Society B: Biological Sciences, 280*(1765), 20130433. https://doi.org/10.1098/rspb.2013.0433

Ichijo, N. (1986). Disjunctive cline of critical photoperiod in the reproductive diapause of *Drosophila lacertosa*. *Evolution*, *40*(2), 418–421. https://doi.org/10.2307/2408820

Johnson, O. L., Tobler, R., Schmidt, J. M., & Huber, C. D. (2023). Fluctuating selection and the determinants of genetic variation. *Trends in Genetics, 39*(6), 491−504. https://doi.org/10.1016/j.tig.2023.02.004

Kim, B. K., Watanabe, T. K., & Kitagawa, O. (1989). Evolutionary genetics of the *Drosophila montium* subgroup. I. Reproductive isolations and the phylogeny. *Japanese Journal of Genetics*, *64*(3), 177–190. https://doi.org/10.1266/jjg.64.177

Kim, D., Paggi, J. M., Park, C., Bennett, C., & Salzberg, S. L. (2019). Graph-based genome alignment and genotyping with HISAT2 and HISAT-genotype. *Nature Biotechnology*, *37*(8), 907–915. https://doi.org/10.1038/s41587-019-0201-4

Kimura, M. T. (1983). Geographic variation and genetic aspects of reproductive diapause in *Drosophila triauraria* and *D. quadraria*. *Physiological Entomology*, *8*(2), 181–186. https://doi.org/10.1111/j.1365-3032.1983.tb00347.x

Kimura, M. T. (1984). Geographic variation of reproductive diapause in the *Drosophila auraria* complex (Diptera: Drosophilidae). *Physiological Entomology*, *9*(4), 425–431. https://doi.org/10.1111/j.1365-3032.1984.tb00784.x

Kimura, M. T. (1987). Habitat differentiation and speciation in the *Drosophila auraria* species-complex (Diptera, Drosophilidae). *Kontyu*, *55*(3), 429−436.

Kimura, M. T. (1988a). Adaptations to temperate climates and evolution of overwintering strategies in the *Drosophila melanogaster* species group. *Evolution*, *42*(6), 1288–1297. https://doi.org/10.1111/j.1558-5646.1988.tb04188.x

Kimura, M. T. (1988b). Interspecific and geographic variation of diapause Intensity and seasonal adaptation in the *Drosophila auraria* species complex (Diptera: Drosophilidae). *Functional Ecology*, *2*(2), 177–183. https://doi.org/10.2307/2389693

Kimura, M. T. (1990). Quantitative response to photoperiod during reproductive diapause in the *Drosophila auraria* species-complex. *Journal of Insect Physiology*, *36*(3), 147–152. https://doi.org/10.1016/0022-1910(90)90115-V

Kimura, M. T., & Yoshida, T. (1995). A genetic analysis of photoperiodic reproductive diapause in *Drosophila triauraria*. *Physiological Entomology*, *20*(3), 253–256. https://doi.org/10.1111/j.1365-3032.1995.tb00009.x

King, R. C. (1970). Ovarian development in *Drosophila melanogaster*. *Academic Press*

Krueger, F. (2015). Trim Galore! [Online]. Available at: https://www.bioinformatics.babraham.ac.uk/projects/trim_galore/

Kozak, G. M., Wadsworth, C. B., Kahne, S. C., Bogdanowicz, S. M., Harrison, R. G., Coates, B. S., & Dopman, E. B. (2019). Genomic basis of circannual rhythm in the European corn borer moth. *Current Biology*, *29*(20), 3501–3509.e5. https://doi.org/10.1016/j.cub.2019.08.053

Kubrak, O. I., Kucerová, L., Theopold, U., Nylin, S., & Nässel, D. R. (2016). Characterization of reproductive dormancy in male *Drosophila melanogaster*. *Frontiers in Physiology*, *7*, 572. https://doi.org/10.3389/fphys.2016.00572

Kumar, S., Stecher, G., & Tamura, K. (2016). MEGA7: Molecular evolutionary genetics analysis version 7.0 for bigger datasets. *Molecular Biology and Evolution*, *33*(7), 1870–1874. https://doi.org/10.1093/molbev/msw054

Lankinen, P. (1986). Geographical variation in circadian eclosion rhythm and photoperiodic adult diapause in *Drosophila littorlis*. *Journal of comparative physiology A*, *159*, 123–142. https://doi.org/10.1007/BF00612503

Lankinen, P., Kastally, C., & Hoikkala, A. (2023). Clinal variation in the temperature and photoperiodic control of reproductive diapause in *Drosophila montana* females. *Journal of Insect Physiology*, *150*, 104556. https://doi.org/10.1016/j.jinsphys.2023.104556

Langmead, B., & Salzberg, S. L. (2012). Fast gapped-read alignment with Bowtie 2. *Nature Methods*, *9*(4), 357–359. https://doi.org/10.1038/nmeth.1923

Láruson, Á. J., Yeaman, S., & Lotterhos, K. E. (2020). The importance of genetic redundancy in evolution. *Trends in Ecology and Evolution*, *35*(9), 809–822. https://doi.org/10.1016/j.tree.2020.04.009

Lee, S. F., Sgro, C. M., Shirriffs, J., Wee, C. W., Rako, L., Heerwaarden, B. V., & Hoffmann, A. A. (2011). Polymorphism in the *couch potato* gene clines in eastern Australia but is not associated with ovarian dormancy in *Drosophila melanogaster*. *Molecular Ecology*, *20*(14), 2973–2984. https://doi.org/10.1111/j.1365-294X.2011.05155.x

Lemeunier, F., David, J., Tsacas, L., & Ashburner, M. (1986). The *melanogaster* species group. genetics and biology of *Drosophila* 3e, *Academic Press*.

Li, H., Handsaker, B., Wysoker, A., Fennell, T., Ruan, J., Homer, N., Marth, G., Abecasis, G., & Durbin, R. (2009). The sequence alignment/map format and SAMtools. *Bioinformatics*, *25*(16), 2078–2079. https://doi.org/10.1093/bioinformatics/btp352

Lindestad, O., Nylin, S., Wheat, C. W., & Gotthard, K. (2022). Local adaptation of life cycles in a butterfly is associated with variation in several circadian clock genes. *Molecular Ecology*, *31*(5), 1461–1475. https://doi.org/10.1111/mec.16331

Lindestad, O., Nylin, S., Wheat, C. W., & Gotthard, K. (2024). Testing for variation in photoperiodic plasticity in a butterfly: Inconsistent effects of circadian genes between geographic scales. *Ecology and Evolution*, *14*(7), e11713. https://doi.org/10.1002/ece3.11713

Low, K. H., Lim, C., Ko, H. W., & Edery, I. (2008). Natural variation in the splice site strength of a clock gene and species-specific thermal adaptation. *Neuron*, *60*(6), 1054–1067. https://doi.org/10.1016/j.neuron.2008.10.048

Majercak, J., Sidote, D., Hardin, P. E., & Edery, I. (1999). How a circadian clock adapts to seasonal decreases in temperature and day length. *Neuron*, *24*(1), 219–230. https://doi.org/10.1016/S0896-6273(00)80834-X

Manning, L., Sheth, J., Bridges, S., Saadin, A., Odinammadu, K., Andrew, D., Spencer, S., Montell, D., & Starz-Gaiano, M. (2017). A hormonal cue promotes timely follicle cell migration by modulating transcription profiles. *Mechanisms of Development*, *148*, 56–68. https://doi.org/10.1016/J.MOD.2017.06.003

Mathias, D., Jacky, L., Bradshaw, W. E., & Holzapfel, C. M. (2005). Geographic and developmental variation in expression of the circadian rhythm gene, *timeless*, in the pitcher-plant mosquito, *Wyeomyia smithii*. *Journal of Insect Physiology*, *51*(6), 661–667. https://doi.org/10.1016/j.jinsphys.2005.03.011

Mayekar, H. V., Ramkumar, D. K., Garg, D., Nair, A., Khandelwal, A., Joshi, K., & Rajpurohit, S. (2022). Clinal variation as a tool to understand climate change. *Frontiers in Physiology*, *13*, 880728. https://doi.org/10.3389/fphys.2022.880728

McDonald, M. J., Rosbash, M., & Emery, P. (2001). Wild-type circadian rhythmicity is dependent on closely spaced E boxes in the *Drosophila timeless* promoter. *Molecular*

and Cellular Biology, *21*(4), 1207–1217. https://doi.org/10.1128/mcb.21.4.1207-1217.2001

Minami, N., & Kimura, M. T. (1980). Geographical variation of photoperiodic adult diapause in *Drosophila auraria*. *The Japanese Journal of Genetics*, *55*(5), 319–324. https://doi.org/10.1266/jjg.55.319

Minh, B. Q., Nguyen, M. A. T., & von Haeseler, A. (2013). Ultrafast approximation for phylogenetic bootstrap. *Molecular Biology and Evolution, 30*(5), 1188–1195. https://doi.org/10.1093/molbev/mst024

Minh, B. Q., Schmidt, H. A., Chernomor, O., Schrempf, D., Woodhams, M. D., von Haeseler, A., & Lanfear, R. (2020). IQ-TREE 2: new models and efficient methods for phylogenetic inference in the genomic era. *Molecular Biology and Evolution*, *37*(5), 1530–1534. https://doi.org/10.1093/molbev/msaa015

Miyake, H., & Watada, M. (2007). Molecular phylogeny of the *Drosophila auraria* species complex and allied species of Japan based on nuclear and mitochondrial DNA sequences. *Genes & Genetic Systems*, 82(1), 77–88. https://doi.org/10.1266/ggs.82.77

Montelli, S., Mazzotta, G., Vanin, S., Caccin, L., Corrà, S., Pittà, C. D., Boothroyd, C., Green, E. W., Kyriacou, C. P., & Costa, R. (2015). *Period* and *timeless* mRNA splicing profiles under natural conditions in *Drosophila melanogaster*. *Journal of Biological Rhythms*, *30*(3), 217–227. https://doi.org/10.1177/0748730415583575

Nanda, S., Defalco, T. J., Hui Yong Loh, S., Phochanukul, N., Camara, N., Doren, M. V., & Russell, S. (2009). Sox100B, a *Drosophila* group E Sox-domain gene, is required for somatic testis differentiation. *Sexual Development*, *3*(1), 26–37. https://doi.org/10.1159/000200079

Nguyen, L. T., Schmidt, H. A., von Haeseler, A., & Minh, B. Q. (2015). IQ-TREE: A fast and effective stochastic algorithm for estimating maximum-likelihood phylogenies. *Molecular Biology and Evolution*, *32*(1), 268–274. https://doi.org/10.1093/molbev/msu300

Oguma, Y., Jallon, J. M., Tomaru, M., Matsubayashi, H. (1996). Courtship behavior and sexual isolation between *Drosophila auraria* and *D. triauraria* in darkness and light, *Journal of Evolutionary Biology*, *9*(6), 803–815. https://doi.org/10.1046/j.1420-9101.1996.9060803.x

Onuma, M., Kamimura, Y., & Sawamura, K. (2022). Genital coupling and copulatory wounding in the *Drosophila auraria* species complex (Diptera: Drosophilidae). *Biological Journal of the Linnean Society*, *135*(1), 195–207. https://academic.oup.com/biolinnean/article/135/1/195/6381422

Ortiz, E. M. (2019) *vcf2phylip v2.0: Convert a VCF matrix into several matrix formats for*

phylogenetic analysis. Zenodo. https://doi.org/10.5281/zenodo.2540861

Paradis, E., & Schliep, K. (2019). ape 5.0: an environment for modern phylogenetics and evolutionary analyses in R. *Bioinformatics*, *35*(3), 526–528. https://doi.org/10.1093/bioinformatics/bty633

Pertea, M., Pertea, G. M., Antonescu, C. M., Chang, T. C., Mendell, J. T., & Salzberg, S. L. (2015). StringTie enables improved reconstruction of a transcriptome from RNA-seq reads. *Nature Biotechnology*, *33*, 290–295. https://doi.org/10.1038/nbt.3122

Pittendrigh, C. S., & Takamura, T. (1987). Temperature dependence and evolutionary adjustment of critical night length in insect photoperiodism. *Proceedings of the National Academy of Sciences of the United States of America*, *84*(20), 7169-7173. https://doi.org/10.1073/pnas.84.20.7169

Pruisscher, P., Nylin, S., Gotthard, K., & Wheat, C. W. (2018). Genetic variation underlying local adaptation of diapause induction along a cline in a butterfly. *Molecular Ecology*, *27*, 3613–3626. https://doi.org/10.1111/mec.14829

Pruisscher, P., Nylin, S., Wheat, C. W., & Gotthard, K. (2021). A region of the sex chromosome associated with population differences in diapause induction contains highly divergent alleles at clock genes. *Evolution*, *75*(2), 490–500. https://doi.org/10.1111/evo.14151

Purcell, S., Neale, B., Todd-Brown, K., Thomas, L., Ferreira, M. A. R., Bender, D., Maller, J., Sklar, P., De Bakker, P. I. W., Daly, M. J., & Sham, P. C. (2007). PLINK: A tool set for whole-genome association and population-based linkage analyses. *The American Journal of Human Genetics*, *81*(3), 559–575. https://doi.org/10.1086/519795

R Core Team (2025). *R: A Language and Environment for Statistical Computing*. R Foundation for Statistical Computing, Vienna, Austria. Available at: https://www.R-project.org/

Rambaut, A. (2018). *FigTree v1.4.4: Tree figure drawing tool*. Institute of Evolutionary Biology, University of Edinburgh. Available at: http://tree.bio.ed.ac.uk/software/figtree/

Rice, G., David, J. R., Kamimura, Y., Masly, J. P., McGregor, A. P., Nagy, O., Noselli, S., Nunes, M. D. S., O'Grady, P., Sánchez-Herrero, E., Siegal, M. L., Toda, M. J., Rebeiz, M., Courtier-Orgogozo, V., & Yassin, A. (2019). A standardized nomenclature and atlas of the male terminalia of *Drosophila melanogaster*. *Fly*, *13*(1–4), 51–64. https://doi.org/10.1080/19336934.2019.1653733

Sandrelli, F., Tauber, E., Pegoraro, M., Mazzotta, G., Cisotto, P., Landskron, J., Stanewsky, R., Piccin, A., Rosato, E., Zordan, M., Costa, R., & Kyriacou, C. P. (2007). A molecular basis for natural selection at the *timeless* locus in *Drosophila melanogaster*. *Science, 316*(5833), 1898–1900. https://doi.org/10.1126/science.1138426

Schliep, K. P. (2011). phangorn: phylogenetic analysis in R. *Bioinformatics*, *27*(4), 592–593. https://doi.org/10.1093/bioinformatics/btq706

Schmidt, P. S., Zhu, C. T., Das, J., Batavia, M., Yang, L., & Eanes, W. F. (2008). An amino acid polymorphism in the *couch potato* gene forms the basis for climatic adaptation in *Drosophila melanogaster*. *Proceedings of the National Academy of Sciences of the United States of America*, *105*(42), 16207–16211. https://doi.org/10.1073/pnas.0805485105

Schneider, C. A., Rasband, W. S., & Eliceiri, K. W. (2012). NIH Image to ImageJ: 25 years of image analysis. *Nature Methods*, *9*, 671–675. https://doi.org/10.1038/nmeth.2089

Sehadova, H., Glaser, F. T., Gentile, C., Simoni, A., Giesecke, A., Albert, J. T., & Stanewsky, R. (2009). Temperature entrainment of Drosophila's circadian clock involves the gene nocte and signaling from peripheral sensory tissues to the brain. *Neuron*, *64*(2), 251–266. https://doi.org/10.1016/j.neuron.2009.08.026

Shafer, O. T., Levine, J. D., Truman, J. W., & Hall, J. C. (2004). Flies by night: effects of changing day length on *Drosophila*'s circadian clock. *Current Biology*, *14*(5), 424–432. https://doi.org/10.1016/j.cub.2004.02.038

Shakhmantsir, I., Nayak, S., Grant, G. R., & Sehgal, A. (2018). Spliceosome factors target *timeless* (*tim*) mRNA to control clock protein accumulation and circadian behavior in *Drosophila*. *eLife*, *7*, e39821. https://doi.org/10.7554/eLife.39821

Shen, W., Sipos, B., & Zhao, L. (2024). SeqKit2: A Swiss army knife for sequence and alignment processing. *iMeta*, *3*, e191. https://doi.org/10.1002/imt2.191

Solares, E. A., Chakraborty, M., Miller, D. E., Kalsow, S., Hall, K., Perera, A. G., Emerson, J. J., & Hawley, R. S. (2018). Rapid low-cost assembly of the *Drosophila melanogaster* reference genome using low-coverage, long-read sequencing. *G3: Genes, Genomes, Genetics, 8*(10), 3143–3154. https://doi.org/10.1534/g3.118.200162

Suzuki, T., Kawai, T., Takemura, S., Nishiwaki, M., Suzuki, T., Nakamura, K., Ishiguro, S., & Higashiyama, T. (2018). Development of the Mitsucal computer system to identify causal mutation with a high-throughput sequencer. *Plant Reproduction*, *31*, 117–128. https://doi.org/10.1007/S00497-018-0331-8

Tapanainen, R., Parker, D. J., & Kankare, M. (2018). Photosensitive alternative splicing of the circadian clock gene *timeless* is population specific in a cold-adapted fly, *Drosophila montana*. *G3: Genes, Genomes, Genetics*, *8*(4), 1291–1297. https://doi.org/10.1534/g3.118.200050

Tauber, E., Zordan, M., Sandrelli, F., Pegoraro, M., Osterwalder, N., Breda, C., Daga, A., Selmin, A., Monger, K., Benna, C., Rosato, E., Kyriacou, C. P., & Costa, R. (2007). Natural selection favors a newly derived *timeless* allele in *Drosophila melanogaster*. *Science*, *316*(5833), 1895–1898. https://doi.org/10.1126/science.1138412

Throckmorton, L. H. (1975). The phylogeny, ecology, and geography of *Drosophila*. In R.C.King (Ed.), *Handbook of Genetics* Vol. 3 (pp. 421–469). *Plenum Press*.

Trivers, R. L. (1972). Parental investment and sexual selection. In B. Campbell (Ed.), *Sexual selection and the descent of man*, 1871–1971 (pp. 136–179), *Aldine*.

Tyukmaeva, V., Lankinen, P., Kinnunen, J., Kauranen, H., & Hoikkala, A. (2020). Latitudinal clines in the timing and temperature-sensitivity of photoperiodic reproductive diapause in Drosophila montana. *Ecography*, *43*, 759–768. https://doi.org/10.1111/ecog.04892

Vaze, K. M., Manoli, G., & Helfrich-Förster, C. (2024). *Drosophila ezoana* uses morning and evening oscillators to adjust its rhythmic activity to different daylengths but only the morning oscillator to measure night length for photoperiodic responses. *Journal of Comparative Physiology A*, *210*, 535–548. https://doi.org/10.1007/s00359-023-01646-6

Watada, M., Matsumoto, M., Kondo, M., & Kimura, M. T. (2011). Taxonomic study of the *Drosophila auraria* species complex (Diptera: Drosophilidae) with description of a new species. *Entomological Science*, *14*, 392–398. https://doi.org/10.1111/j.1479-8298.2011.00461.x

Weir, B. S., & Cockerham, C. C. (1984). Estimating F-statistics for the analysis of population structure. *Evolution*, *38*(6), 1358–1370. https://doi.org/10.2307/2408641

Whitlock, M. C., & McCauley, D. E. (1999). Indirect measures of gene flow and migration: $F_{ST} \neq 1/(4Nm+1)$. *Heredity*, *82,* 117–125. https://doi.org/10.1038/sj.hdy.6884960

Wickham, H. (2016). *ggplot2: Elegant graphics for data analysis*. Springer. https://doi.org/10.1007/978-3-319-24277-4

Willing, E. M., Dreyer, C., & van Oosterhout, C. (2012). Estimates of genetic differentiation measured by F_{ST} do not necessarily require large sample sizes when using many SNP markers. *PLoS ONE*, *7*(8), e42649. https://doi.org/10.1371/journal.pone.0042649

Yamada, H., & Yamamoto, M. (2011). Association between circadian clock genes and diapause incidence in *Drosophila triauraria*. *PLoS ONE*, *6*(12), e27493. https://doi.org/10.1371/journal.pone.0027493

Yu, Y., Huang, L. L., Xue, F. S., & Dopman, E. B. (2023). Partial reuse of circadian clock genes along parallel clines of diapause in two moth species. *Molecular Ecology*, *32*, 3419–3439. https://doi.org/10.1111/mec.16940

Zheng, S., Wang, Y., Li, G., Qin, S., Dong, Z., Yang, X., Xu, X., Fang, G., Li, M., & Zhan, S. (2025). Functional polymorphism of CYCLE underlies the diapause variation in moths. *Science*, *388*(6750), eado2129. https://doi.org/10.1126/science.ado2129

Zonato, V., Fedele, G., & Kyriacou, C. P. (2016). An intronic polymorphism in *couch potato* is not distributed clinally in European *Drosophila melanogaster* populations nor does it

affect diapause inducibility. *PLoS ONE*, *11*(9), e0162370. https://doi.org/10.1371/journal.pone.0162370

Zonato, V., Vanin, S., Costa, R., Tauber, E., & Kyriacou, C. P. (2018). Inverse European latitudinal cline at the *timeless* locus of *Drosophila melanogaster* reveals selection on a clock gene: population genetics of *ls-tim*. *Journal of Biological Rhythms*, *33*(1), 15–23. https://doi.org/10.1177/0748730417742309

Table 1 Strains of *D. triauraria*, *D. auraria*, *D. biauraria*, and *D. subauraria* used in this study.

Species	Strain name	Latitude group	Collection site	Coordinates	Year	Source (fly stock)	Genome accession #
D. triauraria	SPR23-05	High-latitude	Sapporo	43.1°N, 141.2°E	2023	Gift from Masahito T. Kimura.	DRR720568 [f]
D. triauraria	SPR23-09	High-latitude	Sapporo	43.1°N, 141.2°E	2023	Gift from Masahito T. Kimura.	DRR720569 [f]
D. triauraria	TM15-38	High-latitude	Tomakomai	42.6°N, 141.6°E	2015	KYORIN-Fly stock center	DRR720564 [f]
D. triauraria	TM15-57	High-latitude	Tomakomai	42.6°N, 141.6°E	2015	KYOTO *Drosophila* stock center	DRR720565 [f]
D. triauraria	TM15-67	High-latitude	Tomakomai	42.6°N, 141.6°E	2015	KYOTO *Drosophila* stock center	DRR720566 [f]
D. triauraria	TM15-92	High-latitude	Tomakomai	42.6°N, 141.6°E	2015	KYORIN-Fly stock center	DRR720567 [f]
D. triauraria	ONMA20-3	High-latitude	Onuma	42.0°N, 140.4°E	1981	Gift from Shin G. Goto.	DRX055244 [f]
D. triauraria	ONM-15	High-latitude	Onuma	42.0°N, 140.4°E	1984	TMU stock [d]	DRR720577 [f] DRR720578 [f]
D. triauraria	TTR010	Mid-latitude	Tsuchiura	36.1°N, 140.2°E	2017	Collected by M. Onuma (author)	DRR720571 [f]
D. triauraria	T544	Mid-latitude	Tsukuba	36.0°N, 140.0°E	1980	KYORIN-Fly stock center	DRR720570 [f]
D. triauraria	TMU23-02	Mid-latitude	Hachioji	35.6°N, 139.3°E	2023	Collected by T. Fujichika (author)	DRR720572 [f]
D. triauraria	K445	Mid-latitude	Oiso	35.3°N, 139.3°E	1980s [c]	TMU stock [d]	DRR720575 [f] DRR720576 [f]
D. triauraria	Jou	Mid-latitude	Mishima	35.1°N, 138.9°E	1986	TMU stock [d]	DRR720573 [f] DRR720574 [f]
D. triauraria	T748	Mid-latitude	Miyazaki	31.7–32.0°N, 131.2–131.3°E [b]	1982	KYORIN-Fly stock center	SRR13188919
D. triauraria	Yak2	- [a]	Yakushima	30.3°N, 130.6°E	1982	TMU stock [d]	DRR720579 [f] DRR720580 [f]
D. triauraria	Yak3	- [a]	Yakushima	30.3°N, 130.6°E	1982	TMU stock [d]	DRR720581 [f] DRR720582 [f]
D. triauraria	YKS-MTK	- [a]	Yakushima	30.3°N, 130.6°E	1982	KYORIN-Fly stock center	SRR13188918
D. triauraria	OEB12	Low-latitude	Okinoerabu	27.2°N, 128.3°E	2005	KYORIN-Fly stock center	SRR13188921
D. triauraria	OKNG12-6	Low-latitude	Nago	26.7°N, 128.1°E	2012	KYORIN-Fly stock center	SRR13188920
D. triauraria	KMJ1	Low-latitude	Kumejima	26.2°N, 126.5°E	2002	KYORIN-Fly stock center	SRR13188923
D. triauraria	KMJD2	Low-latitude	Kumejima	26.2°N, 126.5°E	2003	KYORIN-Fly stock center	SRR13188922
D. auraria	14028-0471.01	-	Nopporo	43.0°N, 141.5°E	1965	- [e]	SRR9997924
D. auraria	L5	-	Tomakomai	42.6°N, 141.6°E	2011	- [e]	SRR13188915
D. auraria	L8	-	Matsuyama	33.8°N, 132.7°E	2014	- [e]	SRR13188913
D. auraria	L11	-	Matsuyama	33.8°N, 132.7°E	2016	- [e]	SRR13188937
D. biauraria	SPR23-04	-	Sapporo	43.1°N, 141.2°E	2023	Gift from Masahito T. Kimura.	DRR720583 [f]
D. subauraria	ONM-29	-	Onuma	42.0°N, 140.4°E	1982	KYORIN-Fly stock center	DRR720584 [f]

[a] Strains from Yakushima are not assigned to any latitude group.
[b] Exact location unknown.

[c] Exact year of collection unknown.
[d] Stock kept at Tokyo Metropolitan University.
[e] Live flies not used; genomic data only.
[f] Genome sequence data obtained in this study.

Table 2 Results of the linear regression model selected by stepwise BIC for explaining the differences in diapause incidence between light conditions.

Predictor	Estimate (β)	Std. Error	t	P
Intercept	0.813	0.095	8.55	<0.0001
$\Delta_{16L8D\text{-}8L16D}$ *timL*	0.948	0.383	2.47	0.0293

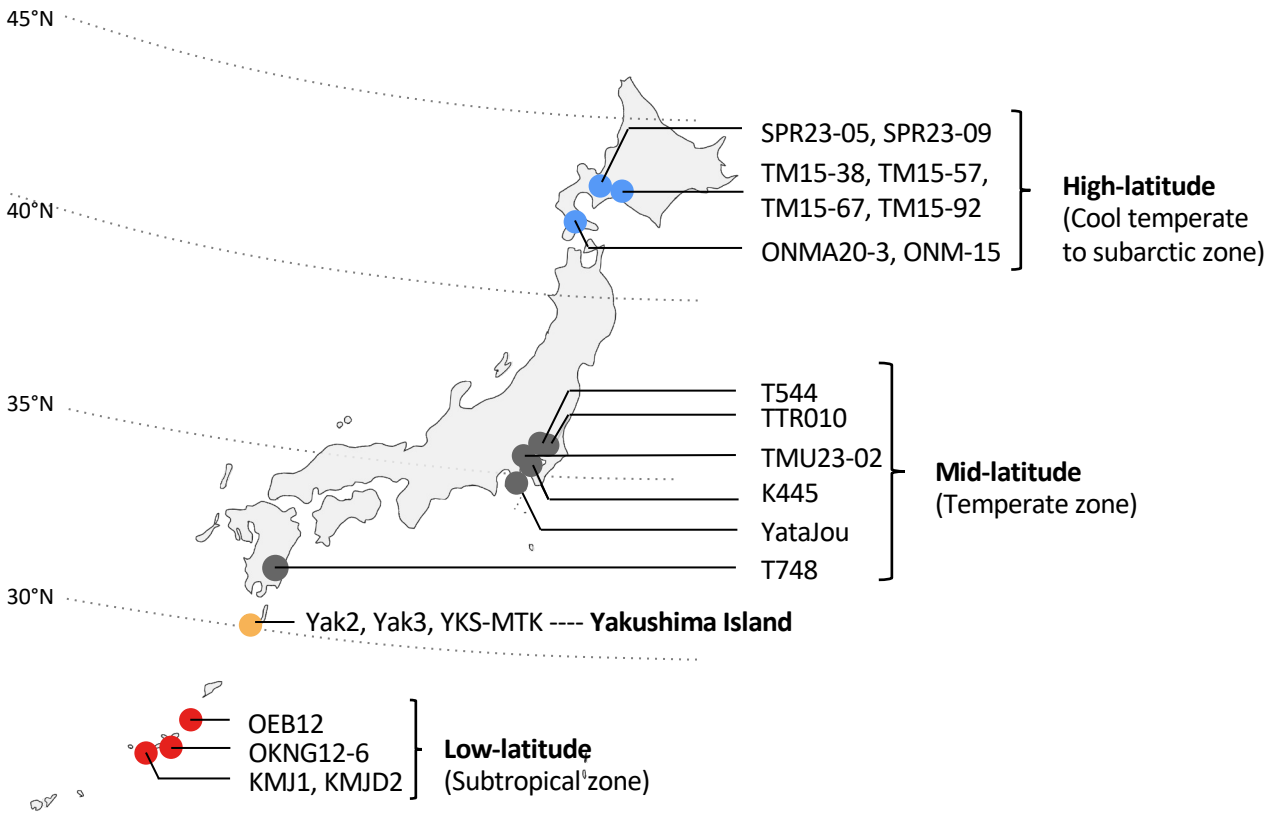

FIGURE 1 Collection sites of *D. triauraria* strains from Japanese archipelago used in this study
A total of 21 isofemale lines of *D. triauraria* that were established from natural populations were used. Circles indicate collection sites: blue, gray, and red denote high-, mid-, and low-latitude regions, respectively, while orange represents Yakushima Island, which has a unique mixed climate distinct from the other regions.

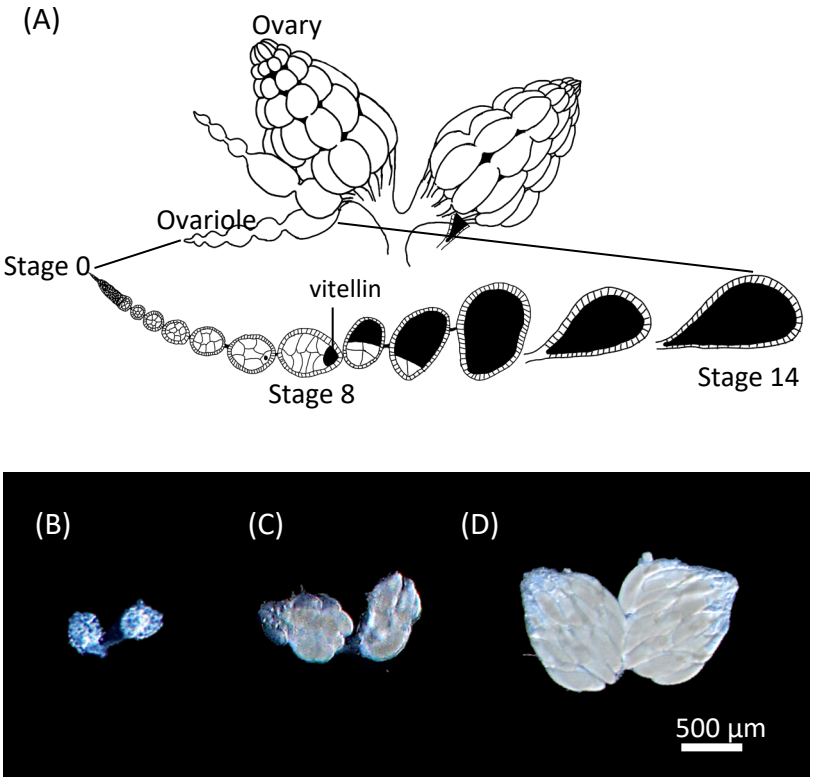

FIGURE 2 Reproductively diapaused and non-diapaused ovaries of *D. triauraria*
(A) Schematic illustration of a pair of *Drosophila* ovaries, modified from King (1970). Each ovary consists of multiple ovarioles, where oogenesis progresses from stage 0 to 14 (mature egg). (B) Diapaused ovaries, lacking eggs at ≥ stage 8 (vitellogenic stages). (C) Non-diapaused ovary with nine eggs at ≥ stage 8. (D) Fully developed ovary.

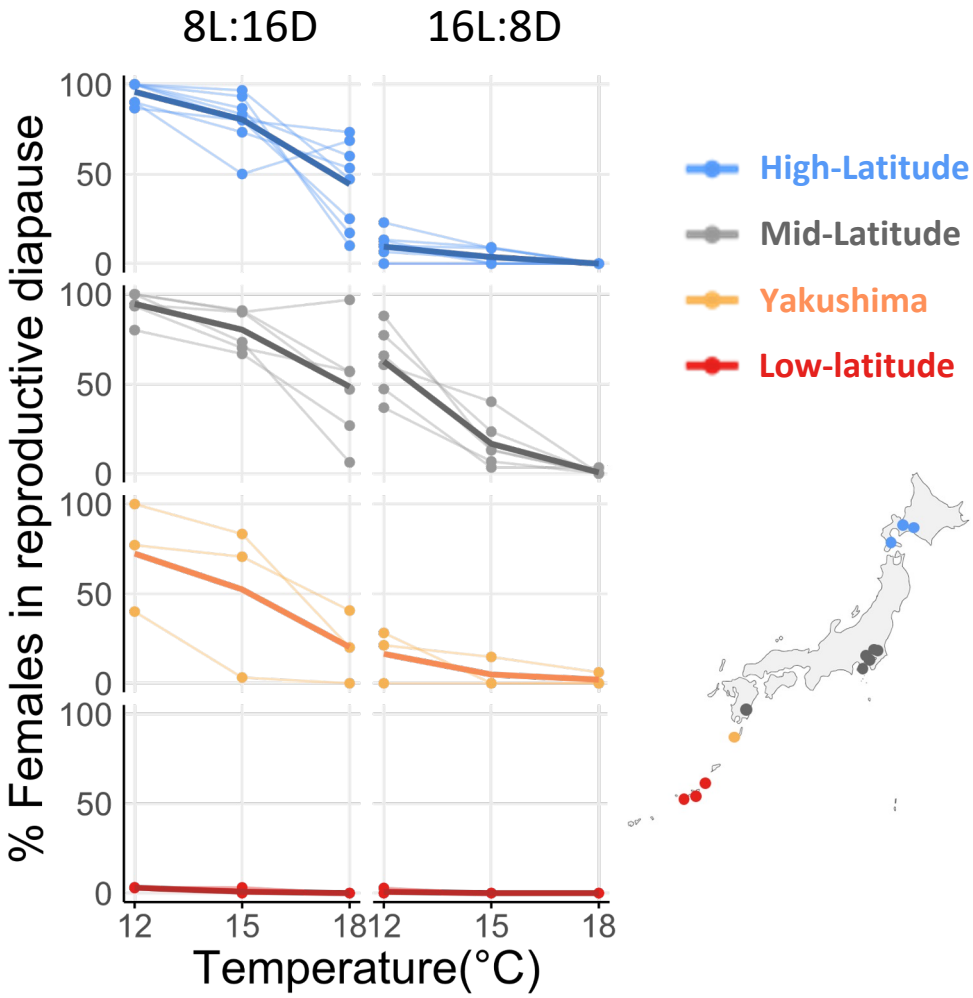

FIGURE 3 Effects of temperature and photoperiod on reproductive diapause incidence across regional populations of *D. triauraria*

The proportion (%) of female individuals in reproductive diapause under different temperatures (12ºC, 15ºC, and 18ºC) and photoperiods (8L:16D or 16L:8D light/dark cycle). The colors indicate different latitudinal regions: blue, grey, orange, and red indicate high-latitude, mid-latitude, Yakushima, and low-latitude regions, respectively. Thick solid line connects the mean at each temperature.

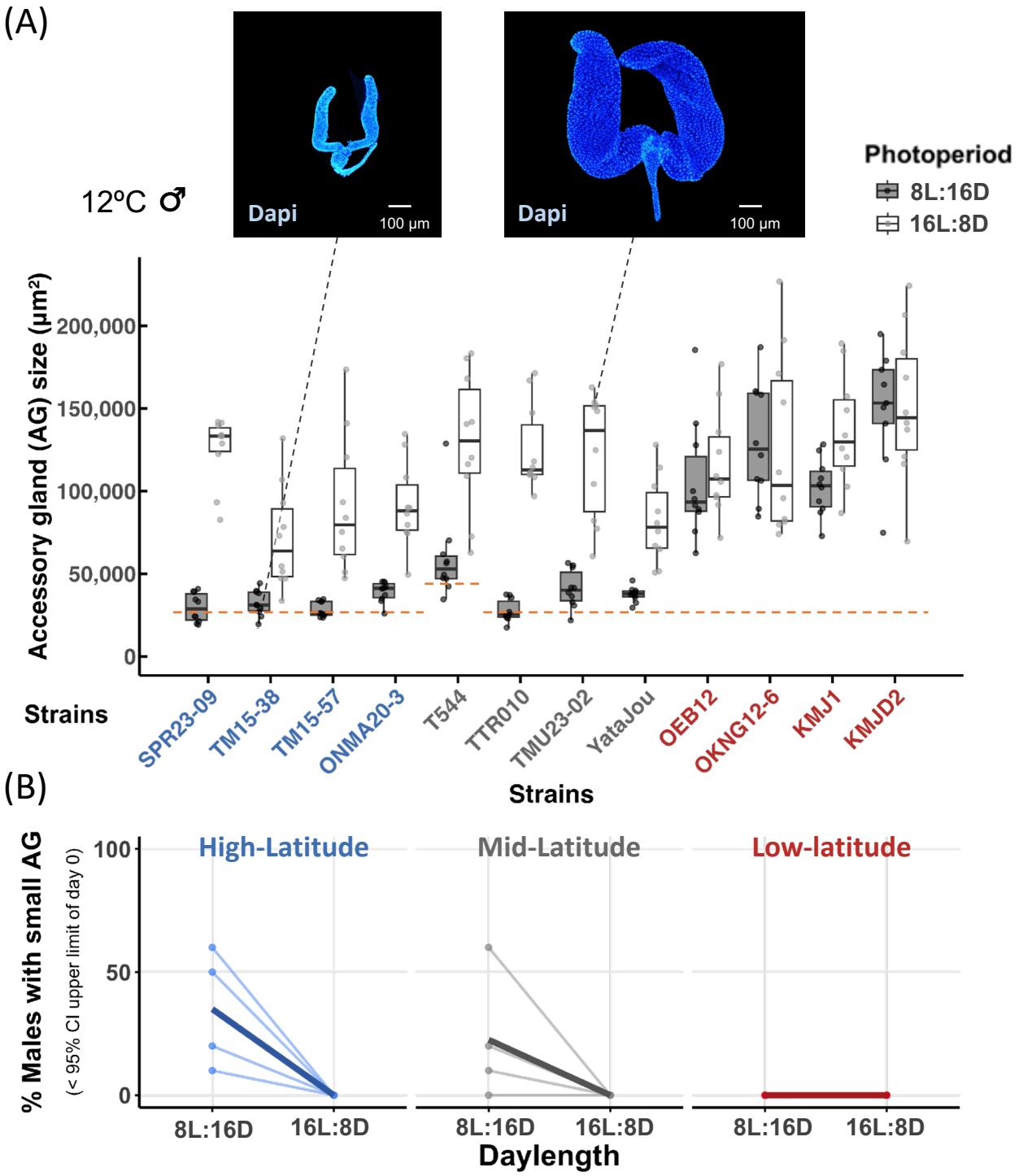

FIGURE. 4 Effects of temperature and photoperiod on accessory gland (AG) growth across regional populations of *D. triauraria*

(A) Sizes of AGs after 21 days under different photoperiods (8L:16D or 16L:8D) at 12ºC. Two representative images of AGs are shown above the graph. Orange dashed lines indicate the upper limit of the 95% CI calculated within strain for T544, and for the remaining strains, from the pooled data excluding T544. The separate calculation for T544 was performed due to its significant difference from other strains (see Figure S1). (B) Proportion (%) of males with AG sizes below the 95% CI upper limit of day 0 after 21 days under 8L:16D or 16L:8D at 12ºC. Colors indicate latitudinal regions: blue, grey, and red indicate high-latitude, mid-latitude, and low-latitude regions, respectively. Thick solid line connects the means at each temperature.

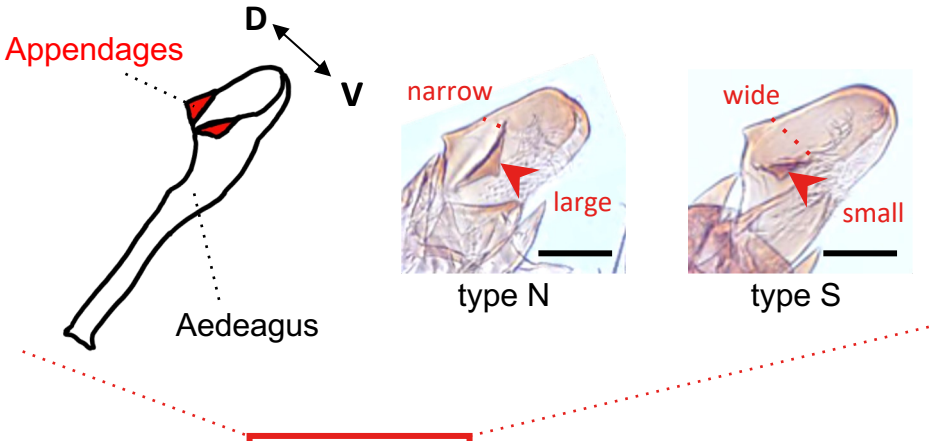

Strain	Aedeagus appendages (N = 10)	Reproductive diapause (%) at 12°C (N = 30–35) 8L16D	16L8D
SPR23-05	type N & S	90	10
SPR23-09	type N & S	86.7	0
TM15-38	type N & S	100	6.5
TM15-57	type N & S	100	10
TM15-67	type N & S	100	22.9
TM15-92	type N & S	100	13.3
ONMA20-3	type N & S	100	12.9
ONM-15	type N & S	90	0
T544	type N & S	100	60.6
TTR010	type S	94.3	77.1
TMU23-02	type N & S	100	47.1
K445	type N & S	80	36.7
Jou	type N & S	100	65.7
T748	type S	93.3	87.9
Yak2	type S	40	0
Yak3	type S	100	28.1
YKS-MTK	type S	77.1	21.2
OEB12	type S	2.9	0
OKNG12-6	type S	3.3	0
KMJ1	type S	2.9	2.9
KMJD2	type S	2.9	0

100%

0%

FIGURE 5 Polymorphism of the aedeagus appendages (dorsolateral claws) compared with female reproductive diapause phenotype in *D. triauraria*

The upper panel shows the scemetic images of the size polymorphism of aedeagus appendages (after Onuma et al. 2022). Scale bar indicates 50 μm. Genital morphology was examined in 10 males per strain and compared with the female reproductive diapause phenotype at 12ºC (lower panel). The colors of the strain names represent their latitudinal regions of origin: blue, grey, orange, and red indicate high-latitude, mid-latitude, Yakushima, and low-latitude regions, respectively.

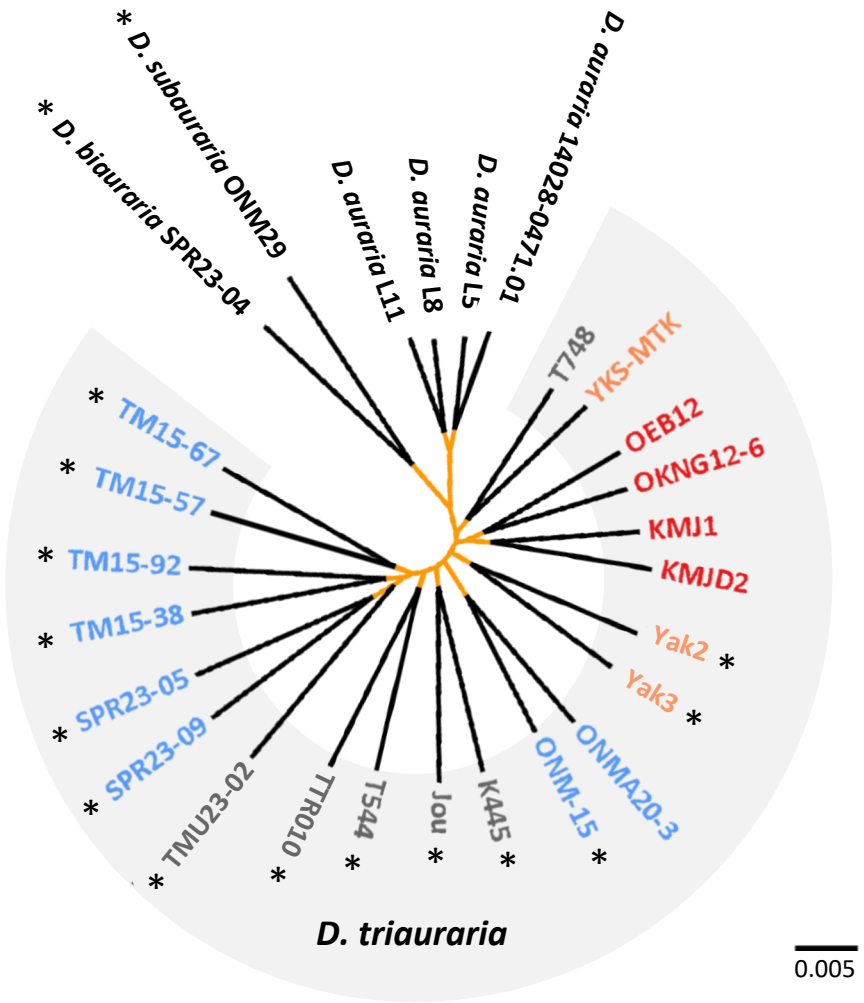

FIGURE 6 Maximum likelihood tree constructed from the whole-genome sequences of *D. triauraria, D. auraria, D. biauraria,* and *D. subauraria* strains used in this study.
Maximum likelihood tree using IQ-TREE with the GTR+G+I model. Nodes with UFBoot value = 100 , estimated from 1,000 pseudo-replicates are highlighted in orange. The colors of *D. triauraria* strain names represent their latitudinal regions of origin: blue, grey, orange, and red indicate high-latitude, mid-latitude, Yakushima, and low-latitude regions, respectively. Asterisks indicate strains whose genomic sequences were obtained in this study.

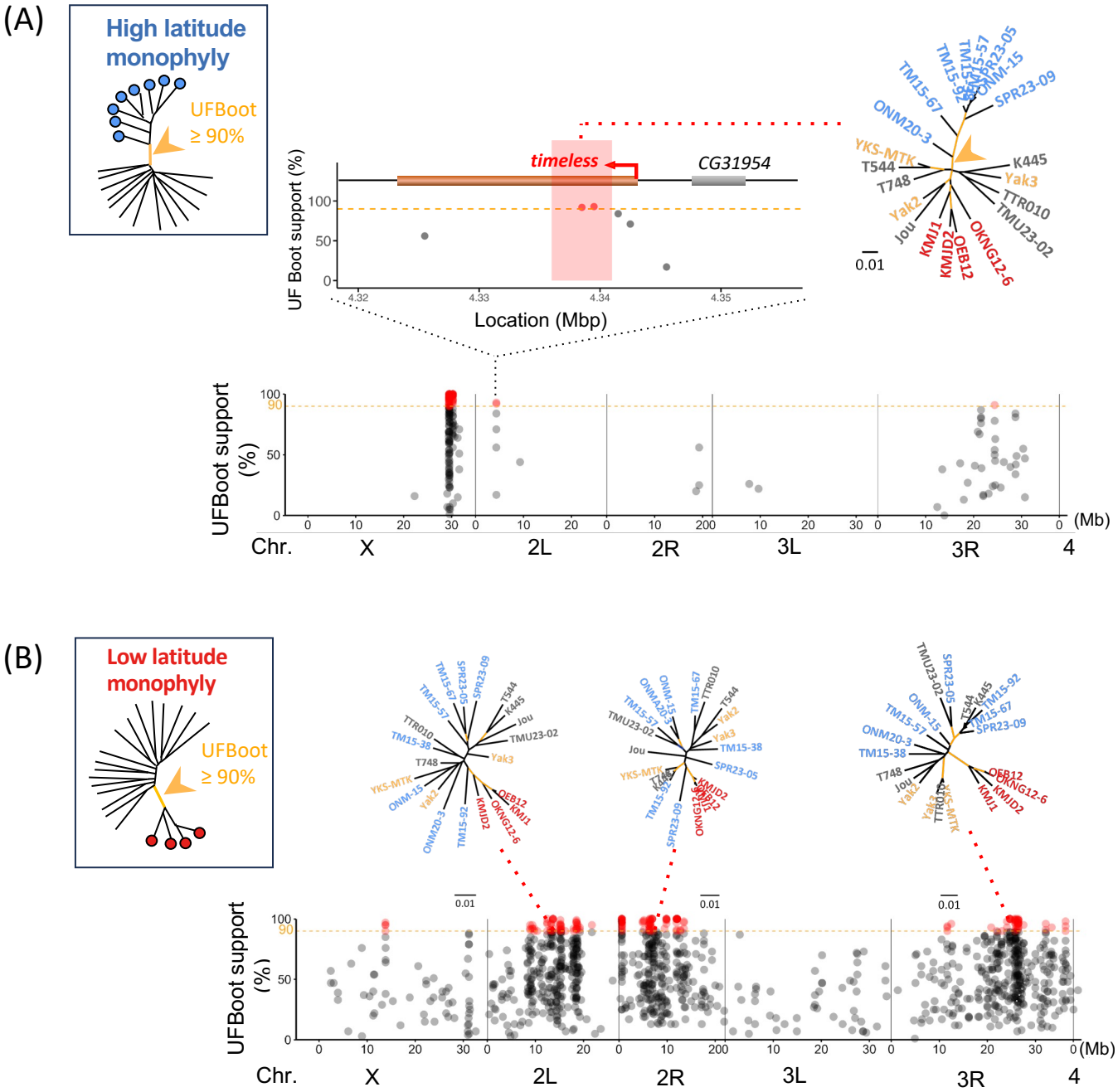

FIGURE 7 Monophyletic window analyses of the high- and low-latitudinal groups.
(A) Sliding window profile of bootstrap (UFBoot) support (%) for monophyly of the high-latitude strain group, based on maximum parsimony trees (window size = 5 kb, step size = 1 kb). Red dots mark the midpoints of windows where the high-latitude strains formed monophyletic clusters with ≥ 90% bootstrap support (1,000 pseudo-replicates). The upper graph zooms in on the region containing the *timeless* (*tim*) gene (brown horizontal bar), which coincides with two consecutive windows above this threshold (midpoints in red). The maximum likelihood tree of one of these windows (highlighted by a pink stripe) is shown, with nodes having UFBoot ≥ 90% highlighted in orange.
(B) Sliding-window profile of bootstrap (UFBoot) support (%) for monophyly of the low-latitude strain group, based on maximum parsimony trees (window size = 5 kb; step size = 1 kb). Red dots mark the midpoints of windows where low-latitude strains formed monophyletic clusters with ≥ 90% bootstrap support (1,000 pseudo-replicates). The maximum likelihood trees of the sampled windows are drawn above the graph, with nodes having UFBoot ≥ 90% highlighted in orange. The genome coordinates are based on the *D. triauraria* reference genome (GCA_014170255.2_RU_Dtri_1.1_genomic.fna). The colors of *D. triauraria* strain names represent their latitudinal origin: blue, grey, orange, and red indicate high-latitude, mid-latitude, Yakushima, and low-latitude regions, respectively.

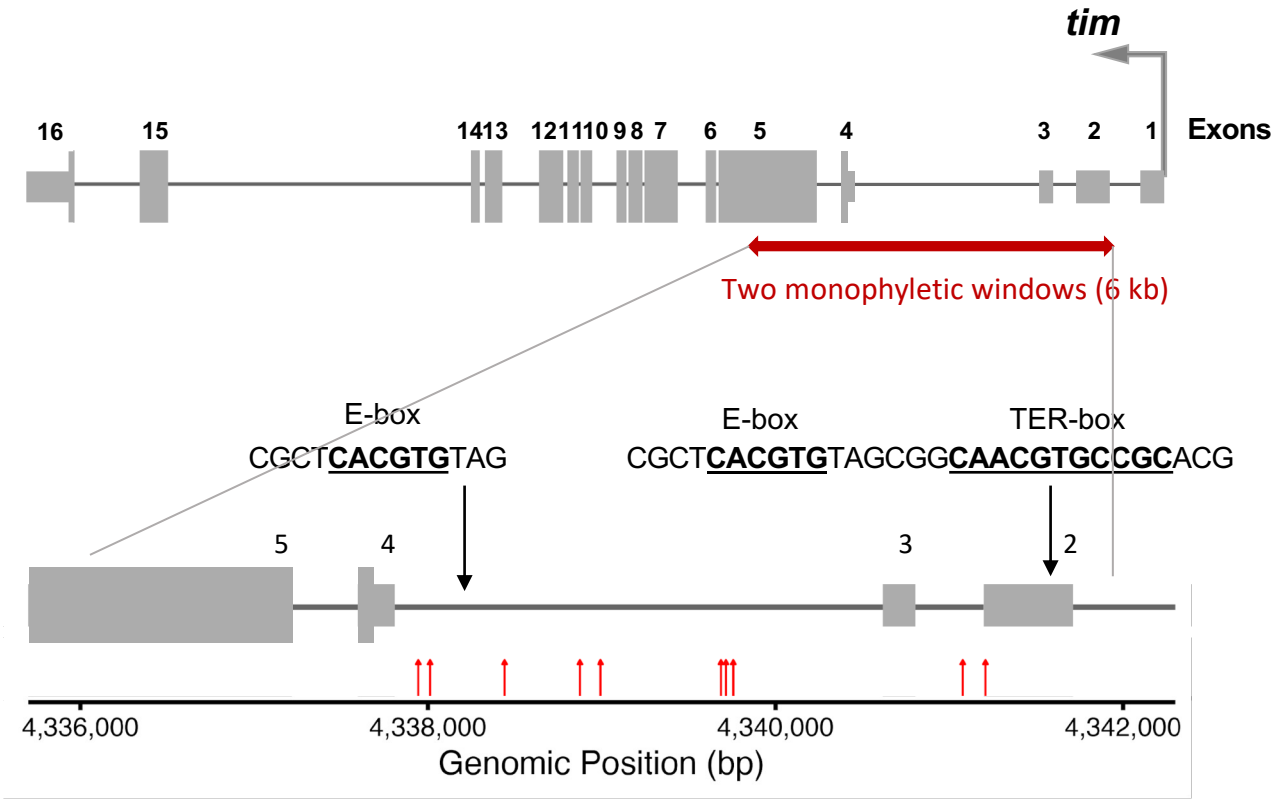

FIGURE 8 Putative E-box and TER-box sequence motifs within the 6 kb region covering the two consecutive monophyletic windows of the high-latitude strains.
The two consecutive monophyletic 5 kb windows are shown in a red horizontal arrow. Gray boxes indicate predicted exons of *tim-L* isoform. Red vertical arrows mark the positions of SNPs that are fixed only in high-latitude populations (positions in bp: 4,337,946, 4,338,013, 4,338,442, 4,338,876, 4,338,994, 4,338,995, 4,339,687, 4,339,715, 4,339,759, 4,341,078, 4,341,209). Putative E-box and TER-box motifs are shown, with the positions corresponding to the indicated sites. The genome coordinates are based on the *D. triauraria* reference genome (GCA_014170255.2_RU_Dtri_1.1_genomic.fna).